SYNTHESIS AND KINETIC EVALUATION OF SUBSTRATES AND INHIBITORS FOR

KYNURENINASE

by

SUNIL KUMAR

(Under the Direction of Robert S. Phillips)

ABSTRACT

Kynureninase is a pyridoxal-5'-phosphate (PLP) dependent enzyme in the kynurenine metabolic pathway of L-tryptophan in animals and bacteria. In mammals, this pathway provides a *de novo* synthesis of $NAD(P)^+$. The mammalian kynureninase catalyses the hydrolytic cleavage of 3-hydroxy-L-kynurenine to 3-hydroxyanthranilic acid and L-alanine. One of the metabolites in this pathway is quinolininc acid. Quinolinic acid is a neurotoxin if produced in excess of its biosynthetic requirement. Potent inhibitors of this enzyme are required as drug targets for several neurological disorders and other diseases including Alzhemier's, AIDS related dementia and Huntington's disease. In the current work, potent inhibitors and substrates for both human and bacterial kynureninase have been synthesized and kinetically evaluated for their enzymatic activity.

INDEX WORDS: Kynureninase, Quinolinic acid, L-tryptophan, PLP, $NAD(P)^+$

SYNTHESIS AND KINETIC EVALUATION OF SUBSTRATES AND INHIBITORS FOR

KYNURENINASE

by

SUNIL KUMAR

B.S., University of Lucknow, 1997

M.S., University of Lucknow, 1999

A Dissertation Submitted to the Graduate Faculty of The University of Georgia in Partial

Fulfillment of the Requirements for the Degree

DOCTOR OF PHILOSOPHY

ATHENS, GEORGIA

2009

SYNTHESIS AND KINETIC EVALUATION OF SUBSTRATES AND INHIBITORS FOR

KYNURENINASE

by

SUNIL KUMAR

Major Professor:	Robert S. Phillips
Committee:	George F. Majetich
	Cory Momany

Electronic Version Approved:

Maureen Grasso
Dean of the Graduate School
The University of Georgia
August 2009

DEDICATION

This dissertation is dedicated to my Guru:

Swami Purushottamanand ji maharaj

And

Swami Chaitanyanand ji

For

their blessings.

ACKNOWLEDGEMENTS

This acknowledgement is incomplete without thanking my past and present group members especially Dr. Vijay Gawandi, Jalandhar Borra, Dr. Chandan Maitrani and Dr. Santiago Lima, Dr. Austin Harris, Dr. Phanneth Som, Quang Trong Do and Kyle beard. I would also like to thank my daily coffee partners Dr. Musa Musa and Johny Do for the interesting morning discussions.

Last but above all I am thankful to my beloved wife Priyanka for providing me unconditional love and emotional support throughout my time in US.

TABLE OF CONTENTS

ABBREVIATIONS

AMPA	α-amino-3-hydroxy-5-methyl-4-isoxazolepropionic acid
AMP	Adenosine monophophate
Arg	Arginine
Asn	Asparginine
ATP	Adenosine triphosphate
Bn	Benzyl
BBB	Blood Brain Barrier
CSF	Cerebrospinal Fluid
CNS	Central Nervous System
DMF	*N,N*-Dimethylformamide
EC	Enzyme Commission
HEPES	4-(2-hydroxyethyl)-1-piperazineethanesulfonic acid
His	Histidine
Hkynase	Human Kynureninase
IDO	Indoleamine 2,3-dioxygenase
IFN	Interferon
IGluRs	Ionotropic glutamate receptors
Ile	Isoleucine
Kyn	Kynurenine
LNAA	Large Neutral Amino Acids

m	multiplet
Me	Methyl
Met	Methionine
mg	milligram
$MgCl_2$	magnesium chloride
$MgSO_4$	magnesium sulfate
mGluRs	metabotropic glutamate receptors
mM	millimolar
mmol	millimole
mV	millivolts
µM	micromolar
NAD+	Nicotinamide Adenine Dinucleotide
NADH	Nicotinamide Adenine Dinucleotide, Reduced
NADP+	Nicotinamide Adenine Dinucleotide Phosphate
NADPH	Nicotinamide Adenine Dinucleotide Phosphate, Reduced
NMDA	N-Methyl-D-Aspartate
NMR	Nuclear Magnetic Resonance
Phe	Phenylalanine
PLP	Pyridoxal-5'-Phosphate
Ppm	parts per million
Ser	Serine
Tris	Tris*(Hydroxymethyl)*aminomethane
TDO	Tryptophan 2,3-dioxygenase

Thr   Threonine

TLC   Thin layer chromatography

Trp   Tryptophan

Tyr   Tyrosine

VDCC   Voltage dependent calcium Channel

Val   Valine

V_{max} maximum velocity

Chapter 1

Introduction and Literature Review

1.1 Kynurenine Pathway

L-Tryptophan is one of the 22 proteinogenic amino acids. In mammals, it is also an essential amino acid i.e., it cannot be synthesized by the body. It is taken as part of the diet and is required by all living cells for protein synthesis. Tryptophan is present in sufficient amounts in protein based foods. The main sources of tryptophan are chocolate, oats, bananas, dried dates, milk, cottage cheese, chicken, fish, turkey, and peanuts. Less is available in corn, cereal grains, legumes (peas and beans), flesh foods, eggs, dairy products, some nuts and seeds and in the casein component of milk. It is a precursor of biologically active compounds like the neurotransmitter, 5-hydroxytryptamine (serotonin) and the neurohormone, melatonin. In our body, tryptophan is extensively bound to plasma albumin and it is the only amino acid that binds to plasma albumin.[1] It exists in equilibrium between albumin–bound (about 90%) and free (about 10%) in the peripheral circulation system. The albumin bound tryptophan cannot cross the blood brain barrier (BBB) but the free form of the tryptophan is available to cross the BBB.[2] The BBB is a regulatory interface between the bloodstream and the brain tissues that inhibit the flow of toxins into the brain, while allowing the admission of essential substances necessary for the function of the brain. All the amino acids can be transported into the brain by facilitated diffusion with the help

of small membrane bound proteins, known as transporters. In a broad sense, there are three types of transporters available to carry different amino acids across the BBB. One is for the large neutral amino acids (LNAA) (Phe, Trp, Met, Ile, Tyr, His, Val, Thr), one is for basic amino acids and the third is for the acidic amino acids. Tryptophan is transported across the blood brain barrier via the L-type amino acid transporters at the luminal and abluminal surface of the endothelial cells.[2] Once the tryptophan crosses BBB and enters the extracellular fluid or cerebrospinal fluid (CSF) of the central nervous system (CNS), it is readily available for uptake into all brain cells for protein synthesis and for other metabolism by different cells, via different pathways. Quantitatively, the most important pathway for tryptophan metabolism after protein synthesis is the kynurenine pathway, which is responsible for over 90% of tryptophan catabolism (Scheme1.1). The initial and rate limiting enzymatic step in the kynurenine pathway is oxidative cleavage of the 2,3-bond of the indole ring of L-Trp. In mammalian liver, the major site for catabolism of L-Trp, this oxidation is performed by a hemeprotein, tryptophan 2,3-dioxygenase (TDO). However, in the extrahepatic cells including the brain cells this reaction is catalyzed by a different hemeprotein, indoleamine 2,3-dioxygenase IDO-1 (or IDO-2[3, 4], a newly discovered enzyme which has same enzymatic activity as IDO-1).

The catalysis by IDO involves the addition of oxygen across the C-2/C-3 double bond of the indole ring. It coordinates molecular oxygen to a heme iron in the ferrous oxidation state. Only the ferrous oxidation state is catalytically active. Oxidation of the heme iron to the ferric state creates an inactive form of the enzyme that requires reduction prior to tryptophan and oxygen binding.[5] Superoxide dismutase, superoxide reductase and IDO

are the only three enzymes that use superoxide as the substrate, and therefore IDO is also considered as a radical scavenger or an antioxidant for the cells. IDO is absent in liver in a majority of mammal but its presence has been shown in other cells like intestinal cells, lungs, placenta and brain.[6] In the human brain IDO activity has been found in primary astrocytes, microvascular endothelial cells, microglia, and macrophages.[7-9] The role of IDO has not been fully understood but the enzyme is induced in number of pathological conditions including bacterial and viral infections, parasitic infestation and tumor transplantation into allogeneic animals. IDO is up-regulated by some cytokines and inflammatory molecules, like amyloid peptides and human immunodeficiency virus (HIV) proteins,[10, 11] but the soluble cytokine interferon gamma (IFN-γ) is the most potent stimulant of IDO.[12-14] The antiproliferative (ability to hinder cell growth) effect of Interferon γ (IFN-γ) on tumor cells and the ability to inhibit intracellular pathogens such as *Toxoplasma* and *Chlamydia* has been partially attributed to the depletion of L-Trp, as a result of induction of IDO in the intracellular region. Some studies have shown that TDO is also expressed in the cytoplasm of neurons, astrocytes, and endothelial cells but not in microglia. It has also been shown in human primary neurons that there is existence of a regulatory mechanism which balances the expression of TDO and IDO.[9]

The product of either TDO or IDO activity with L-Trp is *N*-formyl-L-kynurenine, which is subsequently deformylated to L-kynurenine by an aryl formamidase (Scheme1.1). Hydroxylation of L-Kynurenine by kynurenine monooxygenase then converts it into 3-hydroxy-L-kynurenine. At this point a pyridoxal 5'-phosphate (PLP) dependent enzyme, kynureninase, reacts with 3-hydroxy-L-kynurenine to produces 3-hydroxyanthranilate

and L-alanine. A nonheme iron dioxygenase then converts 3-hydroxyanthranilate to 2-amino-3-carboxymuconic

Scheme 1.1. The kynurenine pathway of tryptophan metabolism

semialdehyde, which spontaneously cyclizes to form quinolinate. In the hepatic tissues, quinolinate is further used in the *de novo* biosynthesis of NAD(P)+, without dietary requirement for niacin. However, in brain cells the primary metabolite of the kynurenine

pathway of tryptophan metabolism appears to be quinolinic acid, not NAD^+. Quinolinic acid can be neurotoxic if produced in excess of its biosynthetic requirements.

1.2 Role of Quinolinic acid in neurological diseases

Quinolinic acid is a known agonist of the N-methyl-D-aspartate (NMDA) receptor. In the case of certain CNS disorders and other diseases there is an overstimulation of the kynurenine pathway which produces more than required quinolinic acid in the brain and damages the neuron. To date, there is no uptake or removal process that has been demonstrated for quinolinic acid. The excitotoxicity of quinolinic acid has been correlated with the etiology of many neurodegenerative diseases including AIDS related dementia[15-17], Huntington's disease[18-21] and Alzheimer's disease[22-26]. The levels of quinolinate in the brain and cerebrospinal fluid are normally less than 100 nM but only a slight increase in the level of quinolinate can be toxic if the cells are exposed for several hours or weeks.[27-29]. Besides activating the NMDA receptor, quinolinic acid can itself be toxic as it can produce free radicals. This fact is supported by several studies[30, 31] that showed that radical scavangers can reduce the toxicity of quinolinic acid.

1.3 Quinolinic acid toxicity via modulation of NMDA receptors

L-Glutamate is the most abundant neurotransmitter in the mammalian central nervous system (CNS). It is present in mM concentration in mammalian central grey matter. It is synthesized inside the body by the transamination of α-ketoglutarate, an intermediate in the citric acid cycle. It is stored in vesicles inside the presynaptic side of a synapse and is released in the synapse on the arrival of active potential in the presynaptic cell. The release of the neurotransmitter is regulated by voltage dependent calcium channels (VDCC) (Figure 1.1).

In Figure 1.1;

A : Neuron (Presynaptic)   B : Neuron (Postsynaptic)

1. Mitochondria

2. Synaptic vesicle full of neurotransmitter

3. Autoreceptor

4. Synaptic cleft

5. Neurotransmitter receptor

6. Calcium Channel

7. Fused vesicle releasing neurotransmitter

8. Neurotransmitter re-uptake pump
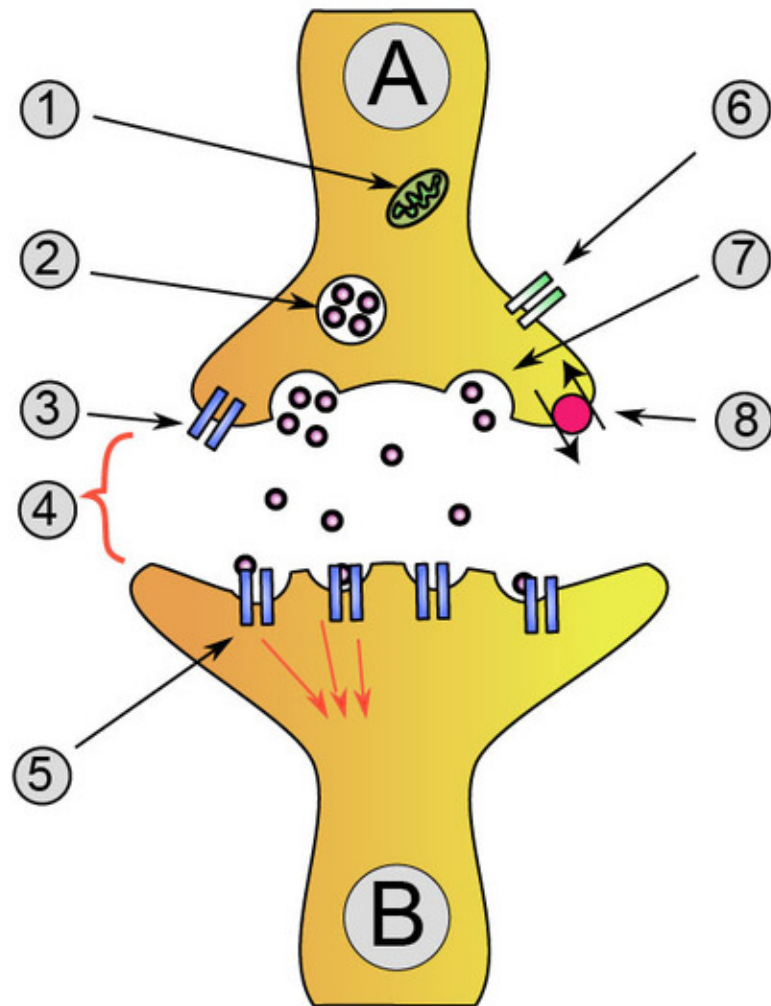
Figure 1.1. A cartoon representation of presynaptic and postsynaptic neuron.

Source: http://en.wikipedia.org/wiki/File:Synapse_diag1.png

Once released to the synapse, glutamate binds to the receptors (so called glutamate receptors) on the membrane of postsynaptic neuron. There are two major types of glutamate receptors, ionotopic glutamate receptors (iGluRs) and metabotropic

glutamate receptors (mGluRs). Ionotropic receptors are further classified in three subfamilies, NMDA (N-methyl-D-aspartate) receptors, AMPA receptors (α-amino-3-hydroxy-5-methyl-4-isoxazolepropionic acid) and kainate receptors (Figure 1.2).
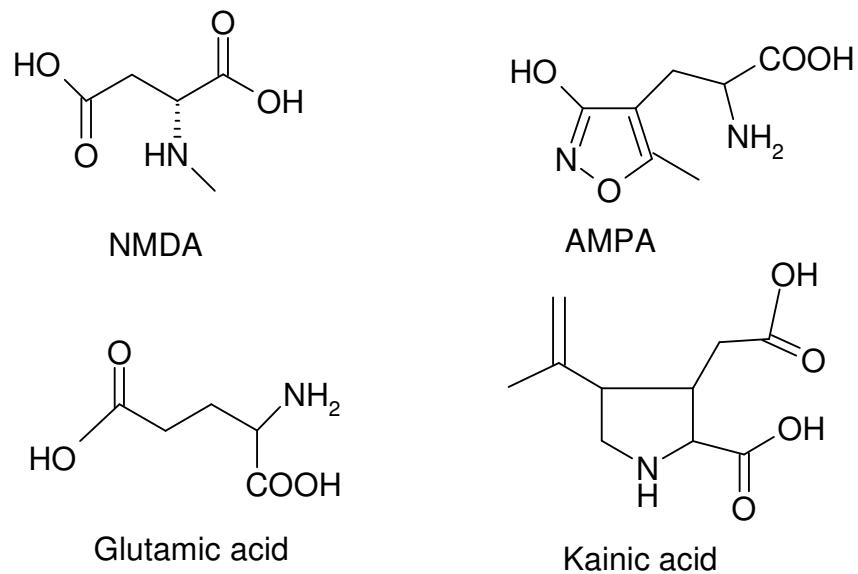
Figure 1.2. Structures of some important amino acids in the brain

Binding of the neurotransmitter may or may not activate the ionotropic recptors depending on the strength of the stimulus in the presynaptic neuron. Most excitatory synapse contains both the NMDA and AMPA receptors (figure 1.3).
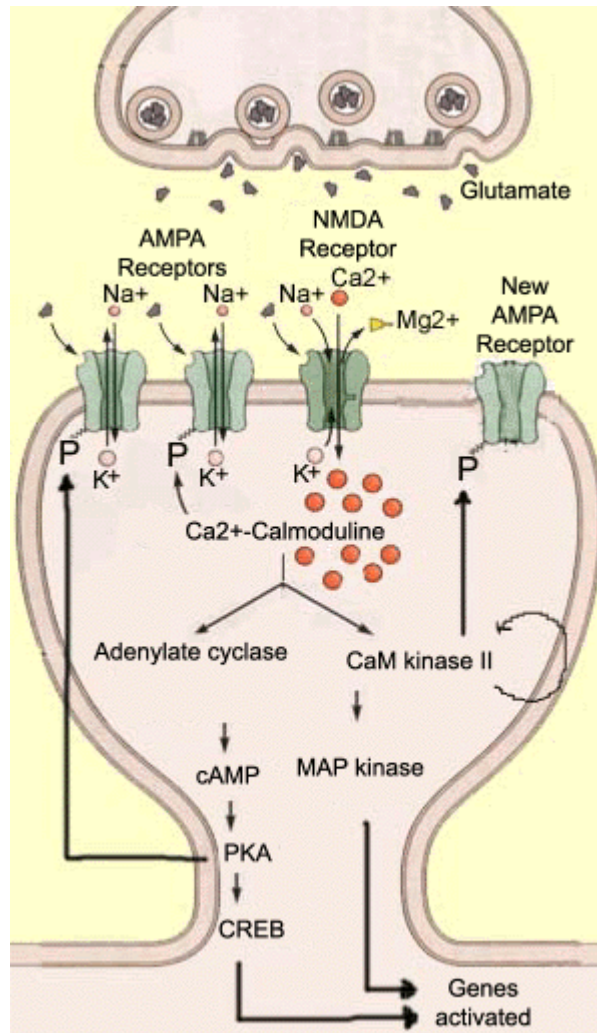
Figure 1.3. A model synapse in the hippocampus containing both types of receptors. (*Source: Brain from top to bottom, picture reproduced under copyleft permission*).

On activation by glutamate, the ionotopic receptors leads to the opening of their associated ion channel which is permeable to Na$^+$, K$^+$, or Ca^{2+} ions depending on the receptor type. For Ionotropic receptors, communication between neurons or cell-signaling occurs primarily by change in ion flux in the extracellular region. Although both receptors are permeable to univalent sodium and potassium ions, weak stimulation

only activates the AMPA receptor, resulting in a slight polarization of the postsynaptic neuron. At slightly depolarized (-35mV) or resting potential (-70mV), binding of glutamate to the NMDA receptor allows only a few ions to enter into the postsynaptic neuron through the NMDA channel. This low conductance occurs because the pore of the NMDA channel is blocked by a magnesium ion (Mg^{2+}) at resting potential, which prevents other ions from passing into the extracellular region. In case of a strong stimulus or frequency in the pre-synaptic neurons, there is a large release of glutamate in the synapse which allows more Na^+ to enter the AMPA receptor. In this case, AMPA receptors can depolarize the membrane sufficiently to expel the Mg^{2+} from the NMDA channel and allow the influx of not only the Na^{2+} ions but also the Ca^{2+} ions through the NMDA channel. The increased concentration of calcium in the post synaptic neuron sets off several biochemical reactions that results in an increase in the activation time of the post synaptic neuron, a condition known as long term potentiation (LTP). LTP is a mechanism for increasing synaptic strength for prolonged period and is considered as one of the major cellular mechanism responsible for learning and memory.

As stated earlier, in the case of overstimulation of the kynurenine pathway in several neurodegenerative disorders there is an overproduction of quinolinic acid.

Since quinolinic acid is an agonist of the NMDA receptor it follows the same path of cell signaling as by the neurotransmitter L-glutamate and its excess in the brain overstimulates the NMDA channel, allowing more than the required influx of calcium ions inside the cell. The rise in intracellular levels of calcium above a critical threshold triggers a cascade of biochemical reactions that result in prolonged or excessive activation of GluRs and causes neuronal degeneration.[32, 33] *Why is this extra calcium so*

toxic to cells? One of the reasons for this toxicity by calcium influx could be the dysfunction of mitochondria.[34] The increase levels of calcium ions in the postsynaptic neuron induces calcium uptake and accumulation in mitochondria. The loading of Ca^{2+} in mitochondria generates reactive oxygen species (ROS) and inhibits the production of adenosine triphophate (ATP), which eventually leads to neuronal death.[35] This process of excessive stimulation of GluRs and neuronal death is known as Excitotoxicity. Among all the glutamate receptors NMDA, has the highest permeability to calcium ions and the higher regions of excitotoxicity are the cells with higher density of NMDA receptors.

To date, there is no cure but only symptomatic treatments available for most neurological diseases including Alzheimer's. Our goal is to design and synthesize inhibitors of kynureniase as potential drug candidates for the treatment of central nervous (CNS) disorders including but not limited to Alzheimer's, AIDS related dementia and Huntington's diseases.

1.4 Structure and function of the enzyme kynureninase (EC 3.7.1.1)

Kynureninase is a member of the aminotransferase or α-superfamily of pyridoxal-5'-phosphate (PLP) (Figure 1.4) dependent enzymes. This enzyme is present in both eukaryotes and prokaryotes. In humans, It catalyzes the hydrolytic cleavage of 3-hydroxy-L-kynurenine to 3-hydroxyanthranilic acid and L-alanine[36, 37] (Scheme 1.1). In the case of prokaryotes, kynureninase preferentially catalyzes the cleavage of L-kynurenine to anthranilic acid and L-alanine. The reaction is a key step in the catabolism of L-tryptophan by *Pseudomonas fluorescens* and some other bacteria.[38]
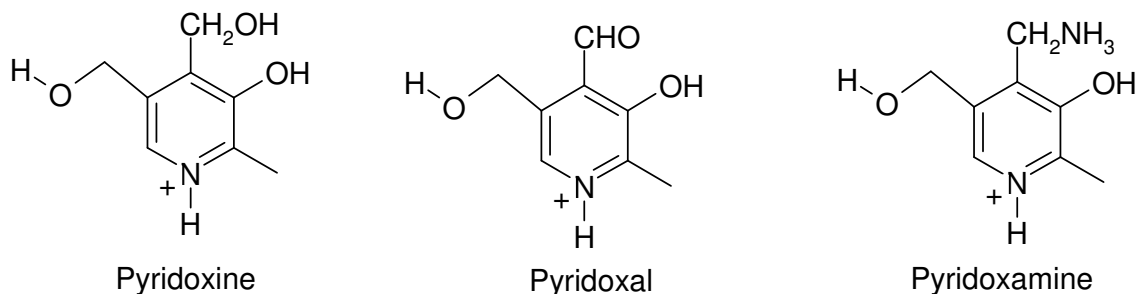
Figure 1.4. Different forms of vitamin B_6

All the reactions of PLP-dependent enzymes start with the formation of imine, or internal aldimine between the aldehyde group of the coenzyme and the nitrogen of the ε-amino of the active site lysine residue. The first step in their reaction with an amino acid substrate is a transimination reaction in which the pyridoxal is transferred from the ε-amino of the lysine to the α-amino of the incoming substrate to form a similar imine, known as external aldimine. The next step is the protonation of the external Schiff base to form an intermediate stabilized by a hydrogen bond. The first few common reaction steps in all PLP-enzymes are shown in scheme 1.2.

It is after the formation of the external aldimine that PLP-dependent enzymes follow different reaction pathways. In a similar manner, the natural substrate, L-kynurenine, and the synthesized substrate, β-benzoyl-L-alanine, react with kynureninase from *Pseudomonas fluorescens* as shown in scheme 1.3. [39]

lysine residue

PLP

Internal aldimine
Schiff base

Amino acid substrate

: NH$_2$-Lys

External aldimine

Amino acid quinonoid

NH$_3$+-Lys
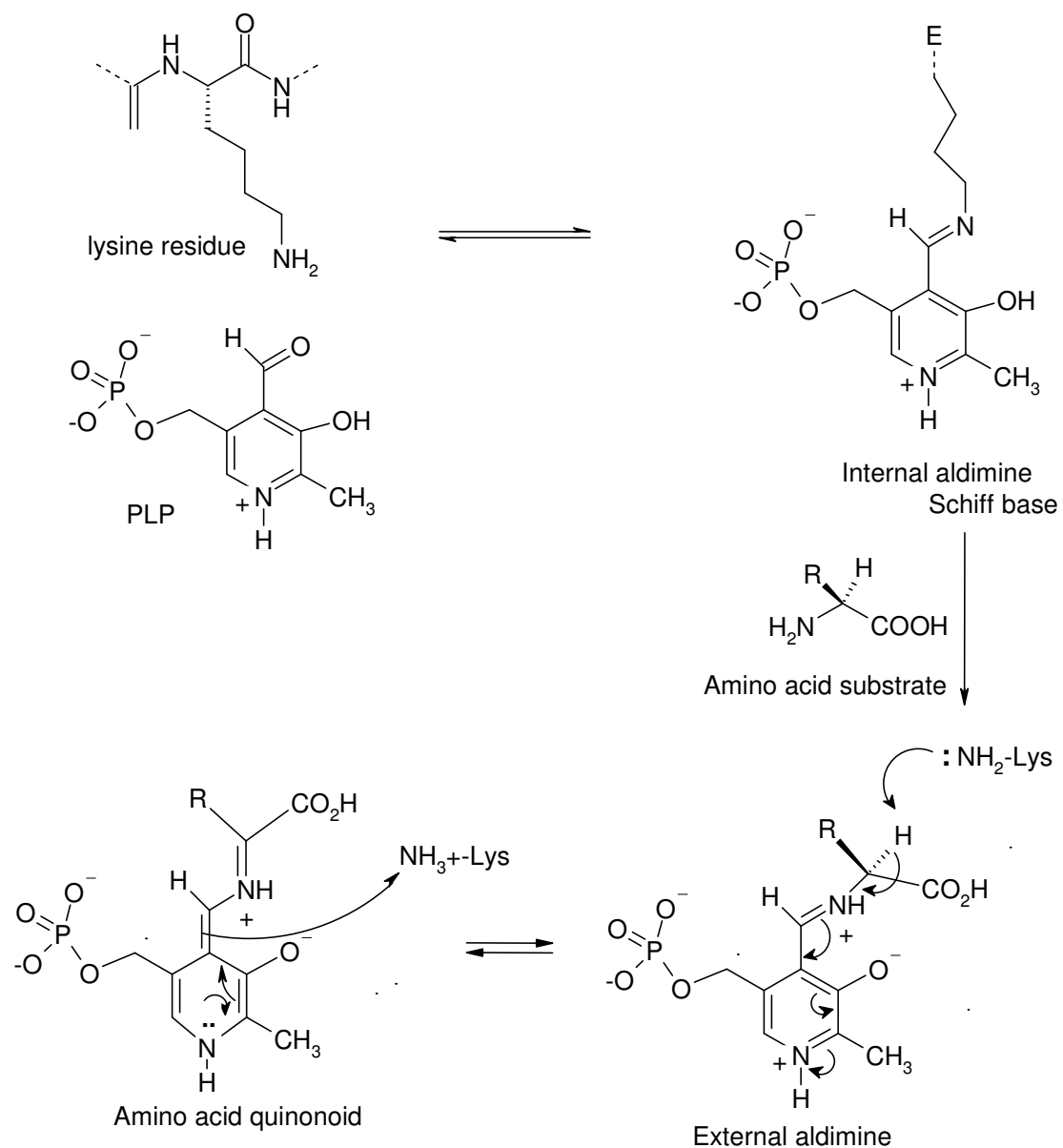
Scheme 1.2. Common steps in all the PLP-dependent enzyme and amino-acid reaction
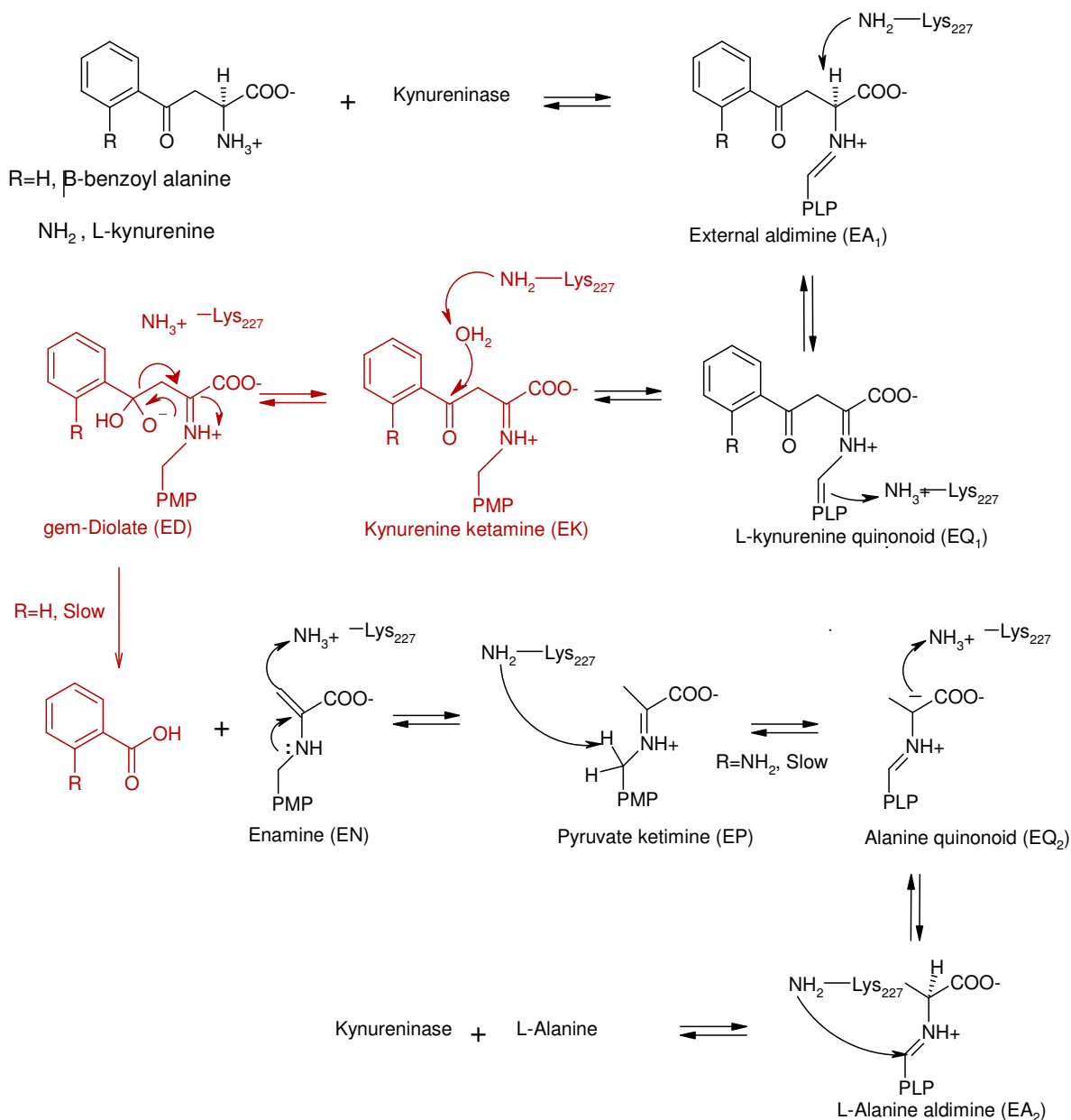
Scheme 1.3. Proposed reaction mechanism for the reaction L-kynurenine and β-benzoylalanine with bacterial kynureninase[39]

According to the above proposed mechanism (Scheme 1.3), β-benzoyl-L-alanine reacts with kynureninase in a similar manner as the natural substrate, L-kynurenine, but the rate limiting steps are different for each substrate. The rate determining step in the reaction of β-benzoyl-L-alanine with kynureninase is C_β–C_γ bond cleavage to form the

first product, benzoate, whereas the rate determining step in the reaction of the natural substrate L-kynurenine with bacterial kynureninase is the release of the second product l-alanine. The k_{cat} for β-benzoyl-L-alanine is identical to the rate constant for the formation of benzoate as seen in the pre-steady state kinetics.

1.5 Refrences

1.	Sainio EL, Pulkki K, Young SN. L-tryptophan: Biochemical, nutritional and pharmacological aspects. Amino Acids, 1996; 10(1):21-47.

2.	Ruddick, J. P.; Evans, A. K.; Nutt, D. J.; Lightman, S. L.; Rook, G. A.; Lowry, C. A., Tryptophan metabolism in the central nervous system: medical implications. *Expert Rev Mol Med* **2006,** 8, (20), 1-27.

3.	Metz, R.; Duhadaway, J. B.; Kamasani, U.; Laury-Kleintop, L.; Muller, A. J.; Prendergast, G. C., Novel tryptophan catabolic enzyme IDO2 is the preferred biochemical target of the antitumor indoleamine 2,3-dioxygenase inhibitory compound D-1-methyl-tryptophan. *Cancer Res* **2007,** 67, (15), 7082-7.

4.	Ball, H. J.; Sanchez-Perez, A.; Weiser, S.; Austin, C. J.; Astelbauer, F.; Miu, J.; McQuillan, J. A.; Stocker, R.; Jermiin, L. S.; Hunt, N. H., Characterization of an indoleamine 2,3-dioxygenase-like protein found in humans and mice. *Gene* **2007,** 396, (1), 203-13.

5.	Sugimoto, H.; Oda, S.; Otsuki, T.; Hino, T.; Yoshida, T.; Shiro, Y., Crystal structure of human indoleamine 2,3-dioxygenase: catalytic mechanism of O2 incorporation by a heme-containing dioxygenase. *Proc Natl Acad Sci U S A* **2006,** 103, (8), 2611-6.

6.	Stone, T. W., Neuropharmacology of quinolinic and kynurenic acids. *Pharmacol Rev* **1993,** 45, (3), 309-79.

7.	Heyes, M. P.; Achim, C. L.; Wiley, C. A.; Major, E. O.; Saito, K.; Markey, S. P., Human microglia convert l-tryptophan into the neurotoxin quinolinic acid. *Biochem J* **1996,** 320 (Pt 2), 595-7.

8. Schroten, H.; Spors, B.; Hucke, C.; Stins, M.; Kim, K. S.; Adam, R.; Daubener, W., Potential role of human brain microvascular endothelial cells in the pathogenesis of brain abscess: inhibition of Staphylococcus aureus by activation of indoleamine 2,3-dioxygenase. *Neuropediatrics* **2001,** 32, (4), 206-10.

9. Guillemin, G. J.; Cullen, K. M.; Lim, C. K.; Smythe, G. A.; Garner, B.; Kapoor, V.; Takikawa, O.; Brew, B. J., Characterization of the kynurenine pathway in human neurons. *J Neurosci* **2007,** 27, (47), 12884-92.

10. Takikawa, O., Biochemical and medical aspects of the indoleamine 2,3-dioxygenase-initiated L-tryptophan metabolism. *Biochem Biophys Res Commun* **2005,** 338, (1), 12-9.

11. Guillemin, G. J.; Smythe, G. A.; Veas, L. A.; Takikawa, O.; Brew, B. J., A beta 1-42 induces production of quinolinic acid by human macrophages and microglia. *Neuroreport* **2003,** 14, (18), 2311-5.

12. Werner-Felmayer, G.; Werner, E. R.; Fuchs, D.; Hausen, A.; Reibnegger, G.; Wachter, H., Characteristics of interferon induced tryptophan metabolism in human cells in vitro. *Biochim Biophys Acta* **1989,** 1012, (2), 140-7.

13. Yasui, H.; Takai, K.; Yoshida, R.; Hayaishi, O., Interferon enhances tryptophan metabolism by inducing pulmonary indoleamine 2,3-dioxygenase: its possible occurrence in cancer patients. *Proc Natl Acad Sci U S A* **1986,** 83, (17), 6622-6.

14. Dai, W.; Gupta, S. L., Regulation of indoleamine 2,3-dioxygenase gene expression in human fibroblasts by interferon-gamma. Upstream control region discriminates between interferon-gamma and interferon-alpha. *J Biol Chem* **1990,** 265, (32), 19871-7.

15. Stone, T. W.; Perkins, M. N., Quinolinic acid: a potent endogenous excitant at amino acid receptors in CNS. *Eur J Pharmacol* **1981,** 72, (4), 411-2.

16. Heyes, M. P.; Brew, B. J.; Martin, A.; Price, R. W.; Salazar, A. M.; Sidtis, J. J.; Yergey, J. A.; Mouradian, M. M.; Sadler, A. E.; Keilp, J.; et al., Quinolinic acid in cerebrospinal fluid and serum in HIV-1 infection: relationship to clinical and neurological status. *Ann Neurol* **1991,** 29, (2), 202-9.

17. Heyes, M. P.; Brew, B.; Martin, A.; Markey, S. P.; Price, R. W.; Bhalla, R. B.; Salazar, A., Cerebrospinal fluid quinolinic acid concentrations are increased in acquired immune deficiency syndrome. *Adv Exp Med Biol* **1991,** 294, 687-90.

18. Heyes, M. P.; Swartz, K. J.; Markey, S. P.; Beal, M. F., Regional brain and cerebrospinal fluid quinolinic acid concentrations in Huntington's disease. *Neurosci Lett* **1991,** 122, (2), 265-9.

19. Haik, K. L.; Shear, D. A.; Schroeder, U.; Sabel, B. A.; Dunbar, G. L., Quinolinic acid released from polymeric brain implants causes behavioral and neuroanatomical alterations in a rodent model of Huntington's disease. *Exp Neurol* **2000,** 163, (2), 430-9.

20. Reynolds, G. P.; Pearson, S. J.; Halket, J.; Sandler, M., Brain quinolinic acid in Huntington's disease. *J Neurochem* **1988,** 50, (6), 1959-60.

21. Foster, A. C.; Whetsell, W. O., Jr.; Bird, E. D.; Schwarcz, R., Quinolinic acid phosphoribosyltransferase in human and rat brain: activity in Huntington's disease and in quinolinate-lesioned rat striatum. *Brain Res* **1985,** 336, (2), 207-14.

22.   Moroni, F.; Lombardi, G.; Robitaille, Y.; Etienne, P., Senile dementia and Alzheimer's disease: lack of changes of the cortical content of quinolinic acid. *Neurobiol Aging* **1986,** 7, (4), 249-53.

23.   Guillemin, G. J.; Williams, K. R.; Smith, D. G.; Smythe, G. A.; Croitoru-Lamoury, J.; Brew, B. J., Quinolinic acid in the pathogenesis of Alzheimer's disease. *Adv Exp Med Biol* **2003,** 527, 167-76.

24.   Mourdian, M. M.; Heyes, M. P.; Pan, J. B.; Heuser, I. J.; Markey, S. P.; Chase, T. N.; Mouradian, M. M., No changes in central quinolinic acid levels in Alzheimer's disease. *Neurosci Lett* **1989,** 105, (1-2), 233-8.

25.   Guillemin, G. J.; Brew, B. J.; Noonan, C. E.; Takikawa, O.; Cullen, K. M., Indoleamine 2,3 dioxygenase and quinolinic acid immunoreactivity in Alzheimer's disease hippocampus. *Neuropathol Appl Neurobiol* **2005,** 31, (4), 395-404.

26.   Guillemin, G. J.; Brew, B. J., Implications of the kynurenine pathway and quinolinic acid in Alzheimer's disease. *Redox Rep* **2002,** 7, (4), 199-206.

27.   Khaspekov, L.; Kida, E.; Victorov, I.; Mossakowski, M. J., Neurotoxic effect induced by quinolinic acid in dissociated cell culture of mouse hippocampus. *J Neurosci Res* **1989,** 22, (2), 150-7.

28.   Kim, J. P.; Choi, D. W., Quinolinate neurotoxicity in cortical cell culture. *Neuroscience* **1987,** 23, (2), 423-32.

29.   Galarraga, E.; Surmeier, D. J.; Kitai, S. T., Quinolinate and kainate neurotoxicity in neostriatal cultures is potentiated by co-culturing with neocortical neurons. *Brain Res* **1990,** 512, (2), 269-76.

30. Nakai, M.; Qin, Z. H.; Wang, Y.; Chase, T. N., Free radical scavenger OPC-14117 attenuates quinolinic acid-induced NF-kappaB activation and apoptosis in rat striatum. *Brain Res Mol Brain Res* **1999,** 64, (1), 59-68.

31. Nakao, N.; Brundin, P., Effects of alpha-phenyl-tert-butyl nitrone on neuronal survival and motor function following intrastriatal injections of quinolinate or 3-nitropropionic acid. *Neuroscience* **1997,** 76, (3), 749-61.

32. Sattler, R.; Tymianski, M., Molecular mechanisms of calcium-dependent excitotoxicity. *J Mol Med* **2000,** 78, (1), 3-13.

33. Sattler, R.; Xiong, Z.; Lu, W. Y.; MacDonald, J. F.; Tymianski, M., Distinct roles of synaptic and extrasynaptic NMDA receptors in excitotoxicity. *J Neurosci* **2000,** 20, (1), 22-33.

34. Nicholls, D. G.; Budd, S. L., Mitochondria and neuronal survival. *Physiol Rev* **2000,** 80, (1), 315-60.

35. Mattson, M. P., Excitotoxic and excitoprotective mechanisms: abundant targets for the prevention and treatment of neurodegenerative disorders. *Neuromolecular Med* **2003,** 3, (2), 65-94.

36. Shetty, A. S.; Gaertner, F. H., Kynureninase-Type enzymes of Penicillum roqueforti, Aspergillus niger, Rhizopus stolonifer, and Pseudomonas fluorescens: further evidence for distinct kynureninase and hydroxykynureninase activities. *J Bacteriol* **1975,** 122, (1), 235-44.

37. Gaertner, F. H.; Shetty, A. S., Hydroxykynureninase and the excretion of 3-hydroxyanthranilate by yeast. *Acta Vitaminol Enzymol* **1975,** 29, (1-6), 332-4.

38.   Soda, K.; Tanizawa, K., Kynureninases: enzymological properties and regulation mechanism. *Adv Enzymol Relat Areas Mol Biol* **1979,** 49, 1-40.

39.   Gawandi, V. B.; Liskey, D.; Lima, S.; Phillips, R. S., Reaction of Pseudomonas fluorescens kynureninase with beta-benzoyl-L-alanine: detection of a new reaction intermediate and a change in rate-determining step. *Biochemistry* **2004,** 43, (11), 3230-7.

CHAPTER 2

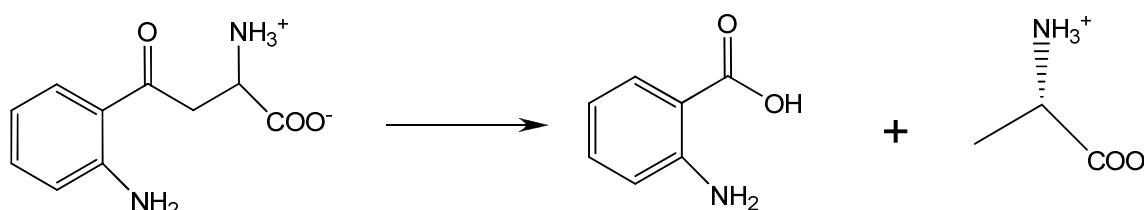## β- Benzoylalanines as Substrates for Bacterial Kynureninase: Synthesis and Kinetic Studies*

2.1 Abstract

β-Benzoyl-L-alanine is a good substrate for kynureninase from *Pseudomonas fluorescens*, with k_{cat} and k_{cat}/K_m values of $0.7 s^{-1}$ and 8×10^4 M^{-1} s^{-1}, respectively, compared to $k_{cat} = 16.0$ s^{-1} and $k_{cat}/K_m = 6.0 \times 10^5$ M^{-1} s^{-1} for L-kynurenine. β-Benzoyl-D-alanine is not a substrate or inhibitor of bacterial kynureninase. A series of β- benzoyl-DL-alanines were synthesized and checked for their substrate activity with bacterial kynureninase from *Pseudomonas fluorescens*. The effect of substitution of β-benzoylalanine with different electron withdrawing and electron donating substituents is also analyzed using a Hammett plot. The Hammett plot suggests that there is a change in rate determining step with different substituents.

2.2 Introduction

Kynureninase (EC 3.7.1.3) is a pyridoxal 5' phosphate (PLP) dependent enzyme that catalyzes the hydrolytic cleavage of L-kynurenine to anthranilic acid and L-alanine [1] (Scheme 2.1). The reaction is a key step in the catabolism of L-tryptophan by *Pseudomonas fluorescens* and some other bacteria,[2] . The kynureninase from *P. fluorescens*, a dimer with a subunit molecular weight of 46483, has been cloned and expressed in *Escherichia coli*.[3] The *P. fluoresens* kynureninase is highly homologous to the human enzyme, with 28% identical residues.[3] In animals and some fungi, a similar constitutive enzyme reacts preferentially with 3-hydroxy-L-kynurenine in the catabolism of L-tryptophan.[1] In these eukaryotes, this pathway is responsible for the biosynthesis of NAD^+, via the intermediacy of quinolinate. However, quinolinate is also a neurotoxin, due to its agonist effects on the *N*-methyl-D-asparate receptor, and excessive levels of quinolinate have been implicated in the etiology of a wide range of diseases such as

epilepsy, stroke, and neurological disorders, including AIDS-related dementia.[4, 5] Thus,

inhibitors of kynureninase are of interest as possible drugs for the treatment of a range

of neurological disorders.[6]

Scheme 2.1. Cleavage of L-kynurenine by kynureninase

It has already been shown that β-benzoyl-L-alanine, which is the desamino form of the

natural substrate, is a good substrate for bacterial kynureninase.[7] β-Benzoyl-L-alanine

has k_{cat} and k_{cat}/K_m values of 0.7 s^{-1} and 8.0 × 10^4 M^{-1} s^{-1}, respectively, compared to k_{cat}

= 16.0 s^{-1} and k_{cat}/K_m = 6.0 × 10^5 M^{-1} s^{-1} for L-kynurenine. The proposed mechanism[7] of

kynureninase reacting with L-kynurenine and β-benzoyl-L-alanine is shown in scheme

2.2. According to the proposed mechanism β-benzoyl-L-alanine reacts with

kynureninase in a similar manner as the natural substrate, L-kynurenine, but the rate

limiting steps are different for each substrate.
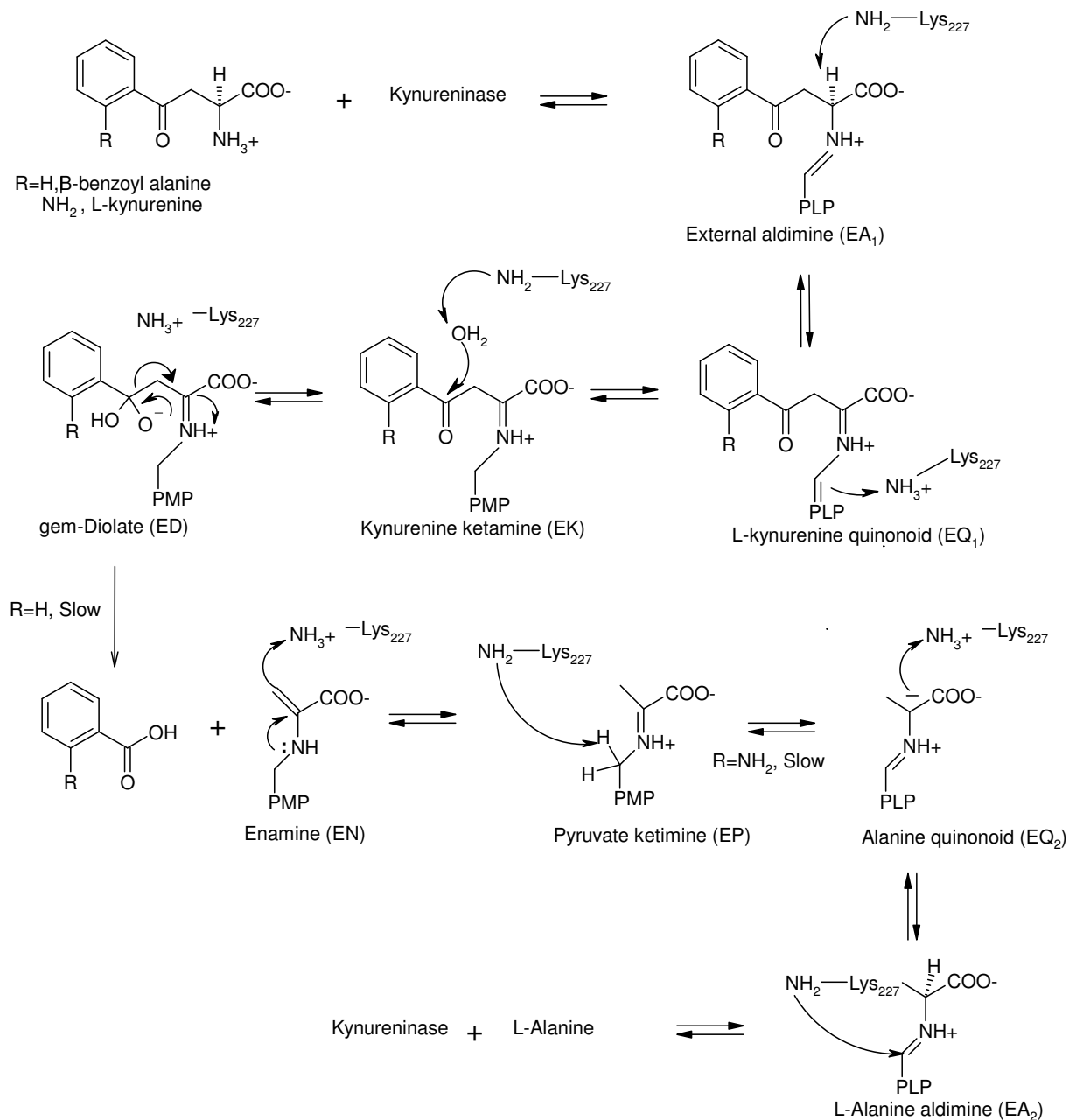
Scheme 2.2. Mechanism of reaction of bacterial kynureninase with β-benzoyl alanine.[7]

The rate determining step in the reaction of β-benzoyl-L-alanine with kynureninase is C_β–C_γ bond cleavage to form the first product, benzoate, where as the rate determining step in the reaction of the natural substrate L-kynurenine with bacterial kynureninase is

the release of the second product alanine. The K_{cat} for β-benzoylalanine is identical to the rate constant for the formation of benzoate as seen in the pre-steady state kinetics.

In the current work, we synthesized a series of substituted β-benzoyl-DL-alanine with electron-withdrawing and electron-donating groups, and checked for their substrate activity with kynureninase. The effects of different substituents on the reaction mechanism with kynureninase is also analyzed using Hammett plots. The results suggest that there is a change in rate determining step with different substituents.

2.3 Results

Chemistry

All of the substituted β-benzoyl-DL-alanine analogs were synthesized based on the procedure by Gawandi *et. al.*[7] The compounds **(1 - 7)** in Figure 2.1 were obtained starting from the alpha bromination of the corresponding substituted acetophenones **(1a - 7a).** Irrespective of the brominating agent used a mixture of mono-brominated and dibrominated acetophenones **(1b – 7b)** were obtained. The monobrominated acetaphenone was separated from the undesired dibrominated product by recrystallization or silica gel column chromatography. Alkylation of the monobrominated acetophenone with diethylacetamidomalonate and sodium hydride as a base afforded alkylated diethyl benzoylmethylacetamidomalonate **(1c – 7c)**. In some cases a mixture of mono- and diester products were obtained along with other unknown byproducts. The alkylated product or products were pooled together and subjected to acid hydrolysis to furnish substituted β-benzoyl-DL-alanine hydrochloride. The amino acid hydrochloride was then converted to the neutral β- benzoyl-DL-alanine **(1 - 7)**.
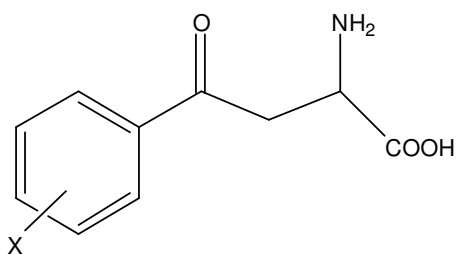
Substrates	Substituents (X)
1	p-OMe-
2	p-Me-
3	p-Cl-
4	p-CF$_3$-
5	o-Cl-
6	o-F-
7	o-OMe-

Fig 2.1 Substituted β-benzoylalanine (X-C_6H_4.CO.CH_2.CH.H_2N.$COOH$)
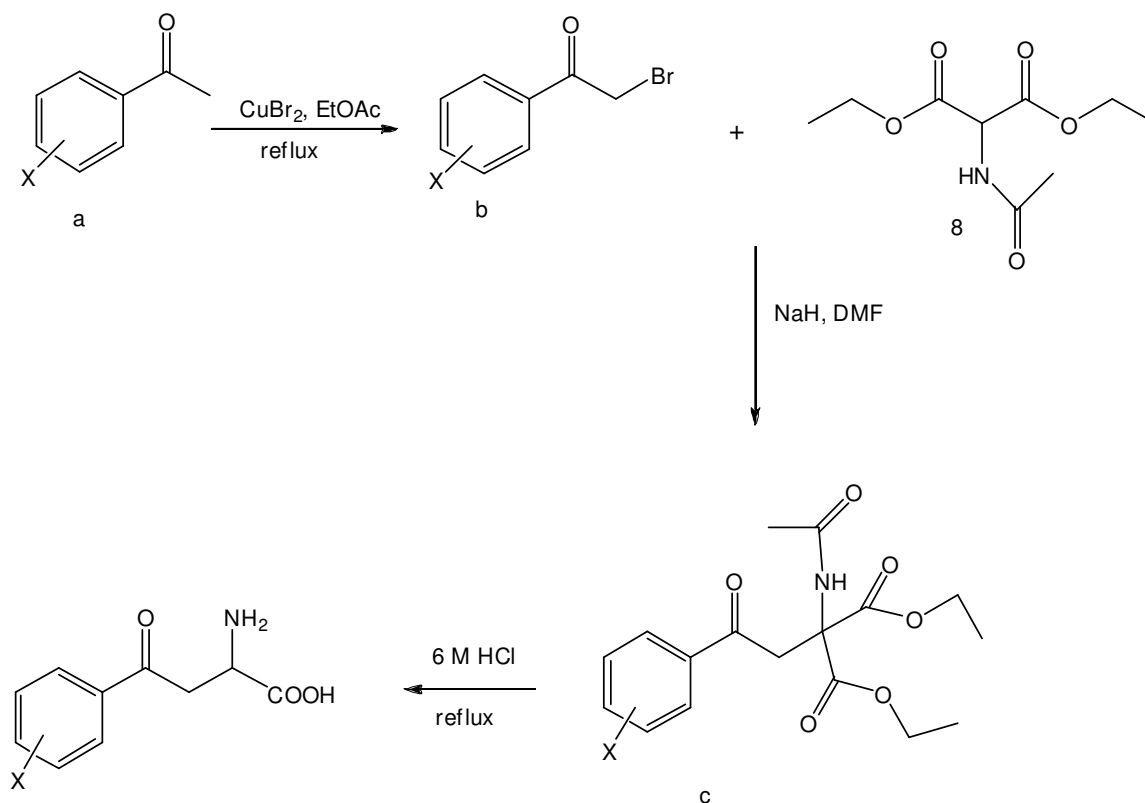
Scheme 2.3. General route for the synthesis of substituted β-benzoylalanine analogs (X-C$_6$H$_4$.CO.CH$_2$.CH.H$_2$N.COOH)

Steady-State Kinetics

The steady state kinetics were performed on a Cary 1E UV/VIS spectrophotometer equipped with a 6 x 6 thermo electric cell changer, controlled by a PC using Windows XP and software provided by Varian instruments. Substrate activities of all the compounds were measured at their absorption maximum. All the assays were done in 0.04 M potassium phosphate, pH = 7.8, containing 40 µM PLP and a total volume of 700 µl.

Table 2.1 Spectroscopic data of substituted β-benzoyl alanines
(X-C$_6$H$_4$.CO.CH$_2$.CH.H$_2$N.COOH)

X-		Molar extinction coefficient	Absorption wavelength (wavelength used for kinetics)
1.	4-OMe-	2600	280
2.	4-Me-	1660	259
3.	4-Cl-	2600	247
4.	4-CF$_3$-	4442	243
5.	2-Cl-	2600	247
6.	2-F-	1946	243
7.	2-OMe-	1504	255

Table 2.2 Kinetic data for substituted β-benzoylalanines

$(X-C_6H_4.CO.CH_2.CH.H_2N.COOH)$

X-	V_{max}	K_m	k_{cat}	k_{cat}/K_m
		(μM)	(s^{-1})	$x\ 10^3\ (M^{-1}s^{-1})$
4-Me-	$(1.3 \pm 0.01)\ x\ 10^{-2}$	32 ± 3.2	0.91 ± 0.06	28 ± 0.02
4-OMe-	$(2.6 \pm 0.01)\ x\ 10^{-2}$	120 ± 31.5	0.38 ± 0.06	1.6 ± 0.28
4-Cl-	$(3.5 \pm 0.1)\ x\ 10^{-2}$	100 ± 6.8	1.83 ± 0.78	18 ± 0.04
4-CF$_3$.	$(8.5 \pm 2.3)\ x\ 10^{-2}$	80 ± 37	$0.001 \pm .0004$	0.019 ± 0.003
2-OMe-	$(0.14 \pm 0.02)\ x\ 10^{-2}$	34 ± 11	0.05 ± 0.006	1.4 ± 0.25
2-Cl-	$(0.4 \pm 0.03)\ x\ 10^{-2}$	6.6 ± 2	0.08 ± 0.006	12 ± 2.8
2-F-	$(0.7 \pm 0.07)\ x\ 10^{-2}$	36 ± 7.7	0.06 ± 0.006	1.7 ± 0.2

V_{max} and V_{max}/K_m values (table 2.2) were all calculated using the FORTAN program

HYPER.
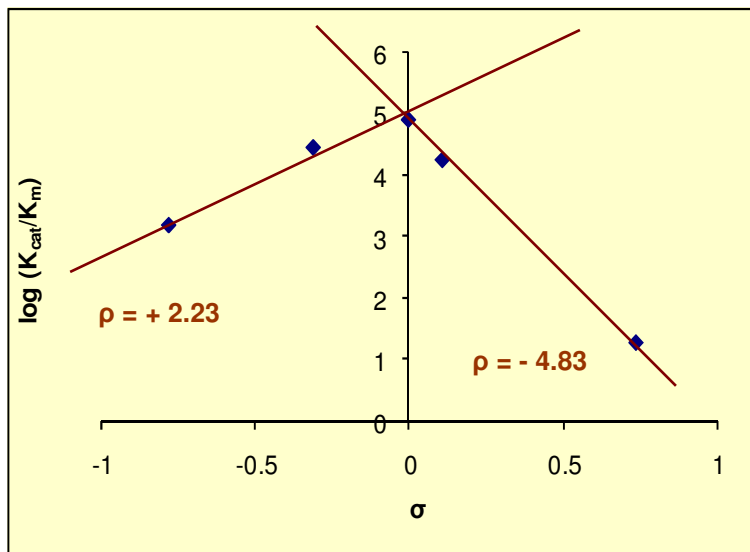
X-	σ	log (k_{cat}/K_m)
p-OMe-	-0.78	3.19
p-Me-	-0.31	4.45
p-H-	0.00	4.9
p-Cl	0.11	4.25
p-CF3	0.74	1.28

Figure 2.2. Hammett Plot of k_{cat}/K_m for p-substituted β-benzoylalanines
(X- $C_6H_4.CO.CH_2.CH.H_2N.COOH$)

σ is the substituent constant. Values of σ are taken from modern physical organic chemistry by Anslyn, E.A. and Dougherty, D.A.
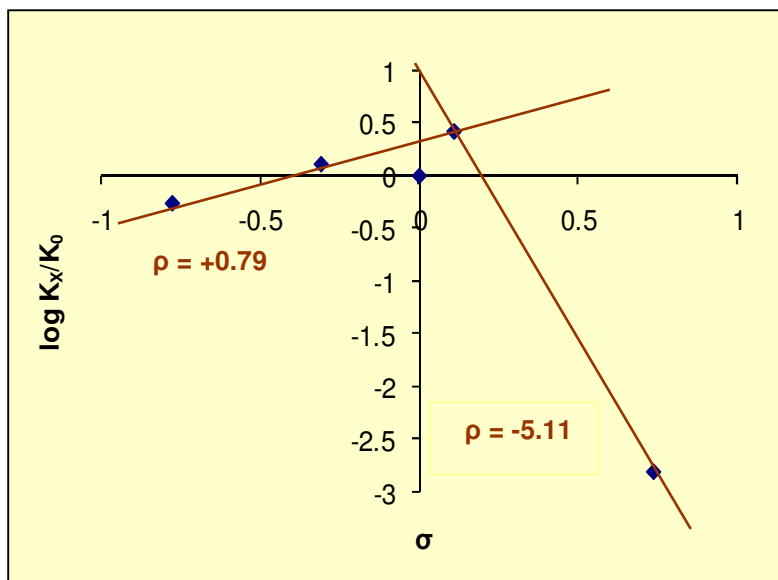
X-	σ	log k_X/k_0
p-OMe-	-0.78	-0.26
p-Me-	-0.31	0.11
p-H-	0	0
p-Cl	0.11	0.42
p-CF3	0.74	-2.8

Figure 2.3. Hammett Plot of substituted β-benzoyl alanines
(X- $C_6H_4.CO.CH_2.CH.H_2N.COOH$).

k_x is the k_{cat} for the substituted benzoylalanines. k_0 is the k_{cat} for the unsustituted benzoyl alanine. σ is the substituent constant

2.4 Discussion

β-Benzoyl-L-alanine is a good substrate for *P. fluorescens* kynureninase. It has been shown that the mechanism of the reaction of β-benzoyl-L-alanine is identical to that of kynurenine, but the rate-limiting step is different for the two substrates. In the case of β-benzoyl-L-alanine the formation of the first product, benzoate is the rate limiting step, whereas with kynureninase the rate-limiting step is the release of the second product, L-alanine. Also, for β-benzoylalanine, k_{cat} is identical to the rate constant for benzoate formation seen in pre-steady-state. In the previous study, it was not clear if the formation of the proposed *gem*-diolate intermediate (ED in Scheme 2.2) or its breakdown is the main contributor to the rate constant for benzoate formation. To resolve the above issue, we synthesized a series of β-benzoylalanine analogs and analyzed their reactivity with kynureninase using a Hammett plot.

In our study of the reaction between kynureninase and different substituted β-benzoylalanines, we obtained a non-linear Hammett plot (Figure 2.2 & 2.3). A non-linear Hammett plot can result from change in the reaction mechanism (upward curvature) or change in the rate determining step (downward curvature).[8] In our study we obtained a downward curve in the Hammett plot of k_{cat}/k_0 against σ which implies a change in the rate determining step with varying substituent. According to the plot, the strong electron-withdrawing substituent CF_3 favors the formation of *gem*-diolate intermediate and hinders the cleavage of the C_β-C_γ bond. The weak electron withdrawing p-Cl which lies at the intersect of two opposite ρ values balances out the hydrolysis of *gem*-diolate and cleavage of C_β-C_γ bond.

Both the electron-donating groups, p-Me and p-OMe, favors the cleavage of C_β-C_γ bond and hinders the attack of water molecule on the carbonyl group in (EK).

The ortho substituted β-benzoylalanines which cannot be analyzed by Hammett plots show moderate activity with the enzyme. The K_m of all the synthesized ortho-substitued analogs are comparable to L-kynurenine, but their low k_{cat} and k_{cat}/K_m values make them slower substrates than the natural substrate, L-kynurenine. As compared to β-benzoylalanine, the ortho-Cl-benzoylalanine has a lower K_m (7 µM) and a comparable k_{cat}/K_m (1.2 x 10^4) against a K_m of 8 µM and k_{cat}/K_m of 8 x 10^4 for β-benzoylalanine.

2.5 Experimental Procedures

Purification of enzyme.

Kynureninase was purified from *Escherichia coli* XL-1 blue cells that were transformed with the pTZKYN plasmid containing the kyn gene cloned from *P. fluorescens.*[3] A single colony of XL-1 Blue cells containing the pTZKYN plasmid was inoculated into 1 L of liquid Luria broth medium containing 100 mg/ml ampicillin and grown overnight at 37 °C with shaking at 225-250 rpm. The cells were centrifuged for 15 min at 5000 *g,* and then suspended in 30 ml buffer (0.05 potassium phosphate, pH 7.0, containing 0.1 mM PLP). The cell suspension was cooled on ice and sonicated for 3 min in 1-min increments with a Branson 300-W sonifier on 50% power. The cell debris were removed by centrifugation for 30 min at 25,000*g* at 4 °C. The supernatant was kept aside at room temperature and then added 4 ml of 2% (w/v) protamine sulfate solution dropwise. The resultant cloudy solution was centrifuged for 30 min at 25000 *g* and 4 °C. The clear supernatant was then brought to 10% saturation with ammonium sulfate by adding solid $(NH_4)_2SO_4$ at 47 °C. The saturated ammonium sulfate solution

containing the desired protein was then loaded on a phenyl-Sepharose (Pharmacia) column (2.5 X 15 cm), which was pre-equilibrated with buffer (0.05 M potassium phosphate, pH 7.0, containing 0.1mM/PLP, 10% saturated with ammonium sulfate). Kynureninase was observed as a bright yellow band adsorbed at the top of the column. The column was then washed with buffer, 5% saturated with ammonium sulfate, at a rate of 60 ml/h for 4 h. Kynureninase was then eluted with potassium phosphate buffer (0.005 M potassium phosphate, pH 7.0, 0.1 mM PLP) and collected in 10 ml fractions. The collected fractions were then assayed for kynureninase activity with L-kynurenine and the ones having the highest activity were pooled together. The resultant solution was brought to a concentration of 0.1 M in buffer by the addition of 1 M potassium phosphate, pH 7.0, and frozen at -78 °C. The concentration of the purified protein was determined using the value of A_{280} = 1.4 mg^{-1} ml^{-1}.[9] and was found to be 14.2 mg/ml.

Synthesis.

4'-Methyl β- benzoyl-DL- alanine.

(2-Amino-4-oxo-4-tolylbutyric acid) (1).

2-Bromo-1-(4-methylphenyl)ethanone (1b). Cupric bromide (3.19 g, 14.2 mmol) was heated at reflux in 10 ml ethyl acetate with stirring. To this was added 4-methylacetophenone (**1a**, 2.36g, 11.4 mmol) in 10 ml chloroform. The reaction mixture was heated at reflux for a further of 5 hrs and then cooled to room temperature. Cuprous bromide and cupric bromide residues were filtered off. The filtrate was decolorized with activated charcoal, filtered through a bed of celite and washed with ethyl acetate (4 x 50 ml). The solvent was removed under reduced pressure to give

yellow crystals. The product was then further purified by recrystallization to give 1.4 g (58%) of the brominated product.

^{1}H NMR (CDCl$_3$) δ (ppm) 2.335 (s, 3H), 4.28 (s, 2H), 7.161 (d, 2H), 7.915 (d, 2H).

Ethyl 4-tolyl-4-oxo-2-acetamido-2-ethoxycarbonylbutyrate (1c).

Sodium hydride (1.39 g, 34.9 mmol, 2.5 equiv) (60% in mineral oil) was suspended in dry DMF (14 ml). A solution of diethyl acetamidomalonate (**8**, 4.56 g, 21 mmol, 1.5 equiv) in dry DMF was added. The solution was stirred at 0 °C under a nitrogen atmosphere for 3 h until the anion had formed. A solution of 2-bromo-1-(4-methylphenyl)ethanone (**1b**, 13.9 mmol, 2.78 g) in dry DMF (10 ml) was added and the solution warmed to room temperature and stirred overnight under nitrogen. The mixture was poured into distilled water (100 ml), acidified to pH 3 with 1 M hydrochloric acid in an ice bath, and extracted into diethyl ether (4 x 70 ml). The ether extracts were dried over MgSO$_4$, and the solvent was removed under reduced pressure to give white crystals of ethyl 4-tolyl-4-oxo-2-acetamido-2-ethoxycarbonylbutyrate (**1c**): Yield, 2.3 g (45%);

^{1}H NMR (CDCl$_3$) δ (ppm) 1.27-1.29 (t, 6H), 1.84 (s, 3H), 2.34 (s, 3H), 3.51 (s, 2H), 4.13 (m, 4H), 7.18 (d, 2H), 7.38 (d, 2H), 7.92 (s, 1H).

 (2-amino-4-oxo-4-tolylbutyric acid) (1).

Ethyl 4-tolyl-4-oxo-2-acetamido-2-ethoxycarbonylbutyrate (**1c**, 1.6 g, 4.7 mmol) was dissolved in 1,4-dioxane (50 ml) and 6 M hydrochloric acid (70 ml) added. The reaction was heated under reflux for 8 h until no starting material was visible by TLC (silica, petroleum ether ethyl acetate; 1:1). The solution was then cooled and washed with ethyl acetate (50 ml). The aqueous phase was concentrated under reduced pressure to give

a brown syrup, which was triturated with acetone to produce 4'-Methyl β- benzoyl-DL-alanine hydrochloride as an off-white crystalline solid. The hydrochloride product was then passed through a cation exchange Dowex 50 column and eluted with 50 ml 1M NH_3 to yield the final compound **(1).** Yield, 0.60 g (65%).

^{1}H NMR (D_2O + DCl) δ (ppm) 2.34 (s, 3H), 3.73-3.74 (dd, 2H), 4.34-4.36 (t, 1H), 7.82 (d, 2H), 7.16 (d, 2H).

4'-Methoxy β- benzoyl-DL- alanine.

2-Amino-4-oxo-4-(4-methoxyphenyl) butyric acid (2).

2-Bromo-1-(4-methoxyphenyl)ethanone (2b). Cupric bromide (3.19 g, 14.2 mmol) was heated at reflux in 10ml ethyl acetate with stirring. To this was added 4'-methoxyacetophenone (**2a**, 2.36 g, 15.7 mmol) in 10 ml chloroform. The reaction mixture was heated at reflux for a further of 5hrs and then cooled to room temperature. Cuprous bromide and cupric bromide residues were filtered off. The filtrate was decolorized with activated charcoal and filtered through a bed of celite and washed with ethyl acetate (4 x 50 ml). The solvent was removed under reduced pressure to give yellow crystals. The product was then further purified by recrystallization with hot ethanol to give 1.9 g (53%) of the brominated product. Mp. 65-69 °C.

^{1}H NMR ($CDCl_3$) δ (ppm) 3.83 (s, 3H), 4.49 (s, 2H), 6.98 (d, 2H), 7.88 (d, 2H).

Ethyl 4-(4-methoxyphenyl)-4-oxo-2-acetamido-2-ethoxycarbonylbutyrate (2c).

Sodium hydride (1.39 g, 34.7 mmol, 2.5 equiv) (60% in mineral oil) was suspended in dry DMF (14 ml). A solution of diethyl acetamidomalonate (**8**, 4.56 g, 21 mmol, 1.5 equiv) in dry DMF was added. The solution was stirred at 0 °C under a nitrogen atmosphere for 3 h until the anion had formed. A solution of 2-bromo-1-(4-

methoxyphenyl)ethanone (**2b**, 13.9 mmol, 3.18 g) in dry DMF (10 ml) was added and the solution warmed to room temperature and stirred overnight under nitrogen. The mixture was poured into distilled water (100 ml), acidified to pH 3 with 1 M hydrochloric acid in an ice bath, and extracted into diethyl ether (4 x 70 ml). The ether extracts were dried over $MgSO_4$, and the solvent was removed under reduced pressure to give white crystals of ethyl 4-(4-methoxyphenyl)-4-oxo-2-acetamido-2-ethoxycarbonylbutyrate **(2c)**. Yield, 2.8 g (55%).

^{1}H NMR (CDCl$_3$) δ (ppm) 1.23-1.27 (t, 6H), 1.88 (s, 3H), 3.89 (s, 3H), 3.51 (s, 2H), 4.15 (m, 4H), 7.01 (d, 2H), 7.88 (d, 2H), 7.8 (s, 1H).

2-Amino-4-oxo-4-(4-methoxyphenyl)butyric acid (2).

 Ethyl 4-(4-methoxyphenyl)-4-oxo-2-acetamido-2-ethoxycarbonylbutyrate (**2c**, 1.71 g, 4.7 mmol) was dissolved in 1, 4-dioxane (50 ml) and 6 M hydrochloric acid (70 ml) added. The reaction was heated under reflux for 8 h until no starting material was visible by TLC (silica, petroleum ether ethyl acetate; 1:1). The solution was then cooled and washed with ethyl acetate (50 ml). The aqueous phase was concentrated under reduced pressure to give a brown syrup, which was triturated with acetone to produce 4'-methoxy- β- benzoyl-DL-alanine hydrochloride as an off-white crystalline solid. The amino acid hydrochloride was then dissolved in water. To the aqueous solution of the amino acid a few drops of acetic acid were added to bring down the pH of the solution to 3. The final product **(2)** was then precipitated by slowly adding ammonium hydroxide solution to the above mixture. Yield 0.62g (60%).

^{1}H NMR (D$_2$O + DCl) δ (ppm) 3.89 (s, 3H), 3.60-3.66 (dd, 2H), 4.28-4.31 (t, 1H), 7.77 (d, 2H), 6.89 (d, 2H).

4'-(Trifluoromethyl)β-benzoyl-DL-alanine.

(2-Amino-4-oxo-4-(4-(trifluromethyl)phenyl)butyric acid) (3).

2-Bromo-1-(4-(trifluoromethyl)phenyl)ethanone (3b). Cupric bromide (4.02 g, 18 mmol) was heated at reflux in 10 ml ethyl acetate with stirring. To this was added 4'-(trifluoromethyl)acetophenone (**3a**, 3.19 g, 16.5 mmol) in 10 ml chloroform. The reaction mixture was heated at reflux for a further 5 hrs and then cooled to room temperature. Cuprous bromide and cupric bromide residues were filtered off. The filtrate was decolorized with activated charcoal and filtered through a bed of Celite and washed with ethyl acetate (4 x 50 ml). The solvent was removed under reduced pressure to give yellow crystals. The product was then further purified by silica gel column chromatography using toluene/hexane (1:9) as solvent. Yield 1.8 g (41%). Mp. 48-56 $^{\circ}$C. ^{1}H NMR (CDCl$_3$) δ (ppm) 4.56 (s, 2H), 7.9 (d, 2H), 7.61 (d, 2H)

Ethyl-4-(4-(trifluoromethyl)phenyl)-4-oxo-2-acetamido-2-ethoxycarbonylbutyrate (3c).

Sodium hydride (1.39 g, 34.7 mmol, 2.5 equiv) (60% in mineral oil) was suspended in dry DMF (14 ml). A solution of diethyl acetamidomalonate (**8**, 4.56 g, 21 mmol, 1.5 equiv) in dry DMF was added. The solution was stirred at 0 ℃ under a nitrogen atmosphere for 3 h until the anion had formed. A solution of 2-bromo-1-(4-(trifluoromethyl)phenyl)ethanone (**3b**, 13.9 mmol, 3.71 g) in dry DMF (10 ml) was added and the solution warmed to room temperature and stirred overnight under nitrogen. The mixture was poured into distilled water (100 ml), acidified to pH 3 with 1 M hydrochloric acid in an ice bath, and extracted into diethyl ether (4 x 70 ml). The ether extracts were dried over MgSO$_4$, and the solvent was removed under reduced pressure to give white

crystals of ethyl 4-(4-trifluoromethyl)phenyl)-4-oxo-2-acetamido-2-ethoxycarbonylbutyrate (**3c**): yield 2.6g (46%);

^{1}H NMR (CDCl$_3$) δ (ppm) 1.25-1.29 (t, 6H), 1.82 (s, 3H), 3.51 (s, 2H), 4.12 (m, 4H), 7.91 (d, 2H), 7.68 (d, 2H), 7.95 (s, 1H).

2-Amino-4-oxo-4-(4-(trifluoromethyl)phenyl)butyric acid (3).

Ethyl-4-(4-(trifluoromethyl)phenyl)-4-oxo-2-acetamido-2-ethoxycarbonylbutyrate (**3c**, 2.6 g, 6.4 mmol) was dissolved in 1, 4-dioxane (50 ml) and 6 M hydrochloric acid (70 ml) added. The reaction was heated under reflux for 8 h until no starting material was visible by TLC (silica, petroleum ether ethyl acetate; 1:1). The solution was then cooled and washed with ethyl acetate (50 ml). The aqueous phase was concentrated under reduced pressure to give white crystals of 4'-trifluoromethyl- β- benzoyl-DL-alanine hydrochloride. The amino acid hydrochloride was then recrystallized from ethanol/water and further subjected to cation exchange on a Dowex-50 column to furnish the free amino acid **(3).** Yield,1.15 g (69%).

^{1}H NMR (D$_2$O + DCl) δ (ppm) 3.56-3.60 (dd, 2H), 4.32-4.35 (t, 1H), 7.97 (d, 2H), 7.68 (d, 2H).

4'-Chloro-β-benzoyl-DL-alanine

(2-amino-4-oxo-4-(4-chlorophenyl)butyric acid) (4).

2-bromo-1-(4-chlorophenyl)ethanone (4b). Cupric bromide (3.19 g, 14.3 mmol) was heated at reflux in 10 ml ethyl acetate with stirring. To this was added 4'-chloroacetophenone (**4a,** 2.21 g, 14.3 mmol) in 10 ml chloroform. The reaction mixture was heated at reflux for a further of 5 hrs and then cooled to room temperature. Cuprous bromide and cupric bromide residues were filtered off. The filtrate was

decolorized with activated charcoal and filtered through a bed of Celite and washed with ethyl acetate (4 x 50 ml). The solvent was removed under reduced pressure to give orange oil. The product was then further purified by recrystallization with ethanol. Yield,1.26 g (41%) of the brominated product.

^{1}H NMR (CDCl$_3$) δ (ppm) 4.56 (s, 2H), 7.42 (d, 2H), 7.86 (d, 2H).

Ethyl 4-(4-chlorophenyl)-4-oxo-2-acetamido-2-ethoxycarbonylbutyrate (4c).

Sodium hydride (1.39 g, 34.9 mmol, 2.5 equiv) (60% in mineral oil) was suspended in dry DMF (14 ml). A solution of diethyl acetamidomalonate (**8**, 4.56 g, 21 mmol, 1.5 equiv) in dry DMF was added. The solution was stirred at 0 ℃ under a nitrogen atmosphere for 3 h until the anion had formed. A solution of 2-bromo-1-(4-chlorophenyl)ethanone (**4b**, 13.9 mmol, 3.24 g) in dry DMF (10 ml) was added and the solution warmed to room temperature and stirred overnight under nitrogen. The mixture was poured into distilled water (100 ml), acidified to pH 3 with 1 M hydrochloric acid in an ice bath, and extracted into diethyl ether (4 x 70 ml). The ether extracts were dried over MgSO$_4$, and the solvent was removed under reduced pressure to give white crystals of ethyl 4-(4-chlorophenyl)-4-oxo-2-acetamido-2-ethoxycarbonylbutyrate **(4c).** The product was further purified by silica gel column chromatography (ethylacetate / hexane) Yield 2.52 g (49%);

^{1}H NMR (CDCl$_3$) δ (ppm) 1.34-1.37 (t, 6H), 1.91 (s, 3H), 3.51 (s, 2H), 4.16 (m, 4H), 7.82 (d, 2H), 7.38 (d, 2H), 7.2 (s, 1H).

(2-Amino-4-oxo-4-(chlorophenyl)butyric acid) (4)..

Ethyl 4-(4-chlorophenyl)-4-oxo-2-acetamido-2-ethoxycarbonylbutyrate (**4b**, 1.73 g, 4.7 mmol) was dissolved in 1,4-dioxane (50 ml) and 6 M hydrochloric acid (70 ml) added.

The reaction was heated under reflux for 8 h until no starting material was visible by TLC (silica, petroleum ether ethyl acetate; 1:1). The solution was then cooled and washed with ethyl acetate (50 ml). The aqueous phase was concentrated under reduced pressure to give a brown syrup, which was triturated with acetone to produce 4'-chloro-β-benzoyl-DL-alanine hydrochloride as an off-white crystalline solid. The hydrochloride product was then passed through a cation exchange Dowex-50 column to yield the final compound **(4).**

Yield 0.650g (61%).

^{1}H NMR (D$_2$O + DCl) δ (ppm) 3.41-3.74 (m, 2H), 4.34-4.36 (t, 1H), 7.82 (d, 2H), 7.4 (d, 2H).

2'-Chloro-β- benzoyl-DL-alanine.

(2-Amino-4-oxo-4-(2-chloro phenyl)butyric acid) (5).

2-Bromo-1-(4-chlorophenyl)ethanone (5a). Cupric bromide (3.19 g, 14.3 mmol) was heated at reflux in 10 ml ethyl acetate with stirring. To this was added 4'-chloroacetophenone (**5a**, 2.21 g, 14.3 mmol) in 10 ml chloroform. The reaction mixture was heated at reflux for a further of 5 hrs and then cooled to room temperature. Cuprous bromide and cupric bromide residues were filtered off. The filtrate was decolorized with activated charcoal and filtered through a bed of celite and washed with ethyl acetate (4 x 50 ml). The solvent was removed under reduced pressure to give an orange oil. The product was then further purified by recrystallization with ethanol. Yield, 1.38 g (45%).

^{1}H NMR (CDCl$_3$) δ (ppm) 4.56 (s, 2H), 7.42 (m, 1H), 7.58 (m, 1H), 7.60 (m, 1H) 7.86 (m, 1H).

Ethyl-4-(2-chlorophenyl)-4-oxo-2-acetamido-2-ethoxycarbonylbutyrate (5c).

Sodium hydride (1.39 g, 34.9 mmol, 2.5 equiv) (60% in mineral oil) was suspended in dry DMF (14 ml). A solution of diethyl acetamidomalonate (**8**, 4.56 g, 21 mmol, 1.5 equiv) in dry DMF was added. The solution was stirred at 0 ℃ under a nitrogen atmosphere for 3 h until the anion had formed. A solution of 2-bromo-1-(2-chlorophenyl)ethanone (**5b**, 13.9 mmol, 3.24 g) in dry DMF (10 ml) was added and the solution warmed to room temperature and stirred overnight under nitrogen. The mixture was poured into distilled water (100 ml), acidified to pH 3 with 1 M hydrochloric acid in an ice bath, and extracted into diethyl ether (4 x 70 ml). The ether extracts were dried over $MgSO_4$, and the solvent was removed under reduced pressure to give white crystals of ethyl 4-(2-chlorophenyl)-4-oxo-2-acetamido-2-ethoxycarbonylbutyrate **(5c).** The product was further purified by silica gel column chromatography (ethyl acetate / hexane)

Yield, 2.98 g (58%).

^{1}H NMR ($CDCl_3$) δ (ppm) 1.34-1.37 (t, 6H), 1.84 (s, 3H), 3.51 (s, 2H), 4.16 (m, 4H), 7.2 (s,1H) 7.41 (m, 1H), 7.57 (s, 1H), 7.52 (s, 1H), 7.91 (s, 1H)

 (2-Amino-4-oxo-4-(2-chlorophenyl)butyric acid) (5).

Ethyl 4-(2-chlorophenyl)-4-oxo-2-acetamido-2-ethoxycarbonylbutyrate (**5c**, 1.73 g, 4.7 mmol) was dissolved in 1,4-dioxane (50 ml) and 6 M hydrochloric acid (70 ml) added. The reaction was heated under reflux for 8 h until no starting material was visible by TLC (silica, petroleum ether ethyl acetate; 1:1). The solution was then cooled and washed with ethyl acetate (50 ml). The aqueous phase was concentrated under reduced pressure to give a brown syrup, which was triturated with acetone to produce

2'-chloro-β- benzoyl-DL-alanine hydrochloride as an off-white crystalline solid. The hydrochloride product was then passed through a cation exchange Dowex-50 column to yield the final compound **(5).**

Yield, 0.72 g (68%).

^{1}H NMR (D$_2$O + DCl) δ (ppm) 3.38-3.44 (m, 2H), 4.35-4.39 (t, 1H), 7.41 (m, 1H), 7.57 (s, 1H), 7.52 (s, 1H), 7.91 (s, 1H).

2'-Fluoro-β-benzoyl-DL-alanine.

(2-Amino-4-oxo-4-(2-fluoro phenyl)butyric acid) (6).

2-Bromo-1-(2-fluorophenyl)ethanone (6b). Cupric bromide (3.19 g, 14.3 mmol) was heated at reflux in 10 ml ethyl acetate with stirring. To this was added 2'-fluoroacetophenone (**6a**, 1.61 ml. 1.96 g, 14.2 mmol) in 10 ml chloroform. The reaction mixture was heated at reflux for a further of 5 hrs and then cooled to room temperature. Cuprous bromide and cupric bromide residues were filtered off. The filtrate was decolorized with activated charcoal, filtered through a bed of celite and washed with ethyl acetate (4 x 50 ml). The solvent was removed under reduced pressure to give a dark yellow oil. Yield, 0.8 g (41%)

^{1}H NMR (CDCl$_3$) δ (ppm) 4.56 (s, 2H), 7.33 (m, 1H), 7.35 (m, 1H), 7.92 (m, 1H) 7.94 (m, 1H).

Ethyl-4-(2-fluorophenyl)-4-oxo-2-acetamido-2-ethoxycarbonylbutyrate (6c).

Sodium hydride (1.39 g, 34.9 mmol, 2.5 equiv) (60% in mineral oil) was suspended in dry DMF (14 ml). A solution of diethyl acetamidomalonate (**8**, 4.56 g, 21 mmol, 1.5 equiv) in dry DMF was added. The solution was stirred at 0 °C under a nitrogen atmosphere for 3 h until the anion had formed. A solution of 2-bromo-1-(2-

fluorophenyl)ethanone (**6b**, 13.9 mmol, 3.01 g) in dry DMF (10 ml) was added and the solution warmed to room temperature and stirred overnight under nitrogen. The mixture was poured into distilled water (100 ml), acidified to pH 3 with 1 M hydrochloric acid in an ice bath, and extracted into diethyl ether (4 x 70 ml). The ether extracts were dried over $MgSO_4$, and the solvent was removed under reduced pressure to give white crystals of ethyl 4-(2-fluorophenyl)-4-oxo-2-acetamido-2-ethoxycarbonylbutyrate **(6c).** The product was further purified by silica gel column chromatography (ethylacetate / hexane)

Yield, 3.18 g (65%);

^{1}H NMR (CDCl$_3$) δ (ppm) 1.36-1.39 (t, 6H), 1.84 (s, 3H), 3.51 (s, 2H), 4.2 (m, 4H), 7.92 (s,1H) 7.95 (m, 1H), 7.93 (m, 1H), 7.32 (m, 1H), 7.30 (m, 1H).

 (2-Amino-4-oxo-4-(2-fluorophenyl)butyric acid*)* **(6).**

 Ethyl-4-(2-fluorophenyl)-4-oxo-2-acetamido-2-ethoxycarbonylbutyrate (**6c**, 1.66 g, 4.7 mmol) was dissolved in 1,4-dioxane (50 ml) and 6 M hydrochloric acid (70 ml) added. The reaction was heated under reflux for 8 h until no starting material was visible by TLC (silica, petroleum ether ethyl acetate; 1:1). The solution was then cooled and washed with ethyl acetate (50 ml). The aqueous phase was concentrated under reduced pressure to give a brown syrup, which was triturated with acetone to produce 2'-fluoro-β-benzoyl-DL-alanine hydrochloride as an white crystalline solid. The hydrochloride product was then passed through a cation exchange Dowex-50 column to yield the final compound **(6).** Yield 0.69g (70%).

^{1}H NMR (D$_2$O + DCl) δ (ppm) 3.38-3.44 (m, 2H), 4.35-4.39 (t, 1H), 7.95 (m, 1H), 7.93 (m, 1H), 7.32 (m, 1H), 7.30 (m, 1H).

2'-Methoxy β- benzoyl-DL- alanine.

2-Amino-4-oxo-4-(2-methoxyphenyl) butyric acid (7).

2-Bromo-1-(2-methoxyphenyl)ethanone (7b). Cupric bromide (3.19 g, 14.2 mmol) was heated at reflux in 10 ml ethyl acetate with stirring. To this was added 2'-methoxyacetophenone (**7a**, 2.13 g, 1.97 ml, 14.2 mmol) in 10 ml chloroform. The reaction mixture was heated at reflux for a further 5 hrs and then cooled to room temperature. Cuprous bromide and cupric bromide residues were filtered off. The filtrate was decolorized with activated charcoal and filtered through a bed of celite and washed with ethyl acetate (4 x 50 ml). The solvent was removed under reduced pressure to give a yellow crystals. The product was then further purified by recrystallization with hot ethanol. Yield 2.01 g (62%) Mp. 43-45 $^\circ$C.

^{1}H NMR (CDCl$_3$) δ (ppm) 3.83 (s, 3H), 4.45 (s, 2H), 7.10 (m, 1H), 7.12 (m, 1H), 7.37 (m, 1H), 7.53 (m, 1H).

Ethyl-4-(2-methoxyphenyl)-4-oxo-2-acetamido-2-ethoxycarbonylbutyrate (7c).

Sodium hydride (1.39 g, 34.7 mmol, 2.5 equiv) (60% in mineral oil) was suspended in dry DMF (14 ml). A solution of diethyl acetamidomalonate (**8**, 4.56 g, 21 mmol, 1.5 equiv) in dry DMF was added. The solution was stirred at 0 °C under a nitrogen atmosphere for 3 h until the anion had formed. A solution of 2-bromo-1-(2-methoxyphenyl)ethanone (**7b**, 13.9 mmol, 3.18 g) in dry DMF (10 ml) was added and the solution warmed to room temperature and stirred overnight under nitrogen. The mixture was poured into distilled water (100 ml), acidified to pH 3 with 1 M hydrochloric acid in an ice bath, and extracted into diethyl ether (4 x 70 ml). The ether extracts were dried over MgSO$_4$, and the solvent was removed under reduced pressure to give white

crystals of ethyl 4-*(4-methoxyphenyl)*-4-oxo-2-acetamido-2-ethoxycarbonylbutyrate (**7c**). Yield, 2.64 g (52%).

^{1}H NMR (CDCl$_3$) δ (ppm) 1.23-1.27 (t, 6H), 1.84 (s, 3H), 3.83 (s, 3H), 3.51 (s, 2H), 4.13 (m, 4H), 7.07 (m, 1H), 7.09 (m, 1H), 7.40 (m, 1H), 7.52 (m, 1H).

7.9 (s, 1H).

2-Amino-4-oxo-4-(2-methoxyphenyl)butyric acid (7).

Ethyl-4-(2-methoxyphenyl)-4-oxo-2-acetamido-2-ethoxycarbonylbutyrate (**7c**, 1.71 g, 4.7 mmol) was dissolved in 1, 4-dioxane (50 ml) and 6 M hydrochloric acid (70 ml) added. The reaction was heated under reflux for 8 h until no starting material was visible by TLC (silica, petroleum ether ethyl acetate; 1:1). The solution was then cooled and washed with ethyl acetate (50 ml). The aqueous phase was concentrated under reduced pressure to give brown syrup, which was triturated with acetone to produce 2'-methoxy-β-benzoyl-DL-alanine hydrochloride as an off-white crystalline solid. The amino acid hydrochloride was then dissolved in water. To the aqueous solution of the amino acid a few drops of acetic acid were added to bring down the pH of the solution to 3. The final product **(7)** was then precipitated by slowly adding ammonium hydroxide solution to the above mixture. Yield, 0.68g (66%).

^{1}H NMR (D$_2$O + DCl) δ (ppm) 3.83 (s, 3H), 3.60-3.66 (dd, 2H), 4.28-4.31 (t, 1H), 7.07 (m, 1H), 7.09 (m, 1H), 7.40 (m, 1H), 7.52 (m, 1H).

2.6 References

1. Soda, K.; Tanizawa, K. *Adv. Enzymol. Relat. Areas Mol. Biol.* **1979,** *49*, 1-40.

2. Hayaishi, O.; Stanier, R. Y. *J. Bacteriol.* **1951***, 62*, 691-709.

3. Koushik, S. V.; Sundaraju, B.; McGraw, R. A.; Phillips, R. S. *Arch. Biochem. Biophysics.* **1997**, 344, 301-308.

4. Achim, C. L.; Heyes, M. P.; Wiley, C. A. *J. Clin. Invest.* **1993**, *91*, 2769-2775.

5. Sei, S.; Saito, K.; Stewart, S. K.; Crowely, J. S.; Brouwers, P.; Kleiner, D. E.; Katz, D. A.; Pizzo, P. A.; Heyes, M. P. *J. Infect. Dis.* **1995***, 172*, 638-647.

6. Stone, T. W.; *Eur. J. Med. Chem.* **2000***, 35*, 179-186.

7. Gawandi, V. B.; Liskey, D.; Lima, S.; Phillips, R. S.; *Biochemistry* **2004,** 43, 3230-3237.

8. Clayden, F. A.; Greeves, N.; Warren, S.; Wothers,S. *Organic Chemistry*, Oxford University Press, USA, **2000**, 1090-1100.

9. Moriguchi, M.; Yamamoto, T.; and Soda, K. *Biochem. Biophys. Res. Commun.* **1971,** *44*, 752-757.

CHAPTER 3

Crystal Structure Of The *Homo sapiens* Kynureninase-3-Hydroxyhippuric Acid Inhibitor Complex: Insights Into The Molecular Basis Of Kynureninase Substrate Specificity*

3.1 Abstract

Homo sapiens kynureninase is a pyridoxal-5′-phosphate dependent enzyme that catalyzes the hydrolytic cleavage of 3-hydroxykynurenine to yield 3-hydroxyanthranilate and L-alanine as part of the tryptophan catabolic pathway leading to the de novo biosynthesis of NAD+. This pathway results in quinolinate, an excitotoxin that is an NMDA receptor agonist. High levels of quinolinate have been correlated with the etiology of neurodegenerative disorders such as AIDS-related dementia and Alzheimer's disease. We have synthesized a novel kynureninase inhibitor, 3-hydroxyhippurate, cocrystallized it with human kynureninase, and solved the atomic structure. On the basis of an analysis of the complex, we designed a series of His-102, Ser-332, and Asn-333 mutants. The H102W/N333T and H102W/S332G/N333T mutants showed complete reversal of substrate specificity between 3-hydroxykynurenine and L-kynurenine, thus defining the primary residues contributing to substrate specificity in kynureninases.

3.2 Introduction

In mammals, the essential amino acid L-tryptophan is a precursor for metabolites such as the neurotransmitter serotonin, the hormone melatonin, nicotinic acid, and NAD+, with the latter two being the primary metabolic fate of dietary tryptophan. The catabolic cascade that leads to the de novo biosynthesis of nicotinic acid and NAD+, commonly known as the kynurenine pathway,[1] is notable for intermediates with important neuroactive properties. Kynureninase, the third enzyme along the kynurenine pathway, is a pyridoxal-5′-phosphate (PLP) dependent enzyme that catalyzes the hydrolytic cleavage of 3-hydroxy-L-kynurenine (3-OH-Kyn) to yield 3-hydroxyanthranilic

acid and L-alanine (Scheme 3.1, R = OH). One further kynurenine pathway enzyme, 3-hydroxyanthranilate-3,4-dioxygenase, metabolizes 3-hydroxyanthranilic acid, the product of which undergoes a nonenzymatic rearrangement leading to the formation of quinolinate.[2] Quinolinate has endogenous neurotoxic activity[3] that is mediated via its agonist effect on glutamate sensitive NMDA ionotropic receptors,[4] and its excitotoxic effect has been correlated with the etiology of many neurodegenerative diseases including AIDS-related dementia,[5,6] Huntington's disease,[7,8] amyotrophic lateral sclerosis,[9] and Alzheimer's disease.[10,11] The increasing body of evidence implicating changes in normal concentrations of quinolinate in CNS tissues with neurotoxicity has led to the idea that altering the ratio of quinolinic acid to other kynurenine pathway metabolites could provide a neuroprotective effect during the onset of such maladies.[12-15] Thus, our goal was to provide a robust template that can be used for rational and in silico drug design as well as complex pharmacophore library screening. Herein we report the crystal structure of *Homo sapiens* kynureninase (HKynase) complexed with

3-hydroxyhippuric acid (**5**), a novel competitive inhibitor of kynureninase. The complex reveals important enzyme-ligand interactions that should be considered for the design and screening of novel kynureninase inhibitors. Two functional orthologues of kynureninase are known, a "constitutive", primarily eukaryotic enzyme[16] that preferentially catalyzes the hydrolysis of 3-OH-Kyn (Scheme3.1,

R = OH) and a primarily prokaryotic "inducible"[16] enzyme that catalyzes the hydrolysis of L-kynurenine (L-Kyn) to yield anthranilic acid and L-Ala (Scheme 3.1, R = H). Although both orthologues are able to catalyze the hydrolysis of their noncognate substrates, they do so at about 100-fold lower efficiency.[17, 18] Indeed, a number of

organisms, especially fungi, are known to contain both orthologues.[16] To date, the molecular basis of the substrate specificity that allows these enzymes to differentiate between their substrates has not been elucidated. Some insight into this mechanism was gained through docking studies with the native structure of *H. sapiens* kynureninase and 3-OH-L-Kyn as the target ligand.18 These results revealed that two active site residues, His-102 and Asn-333, could play an important role in substrate binding and specificity.[18] We present herein additional experimental evidence supporting this hypothesis.
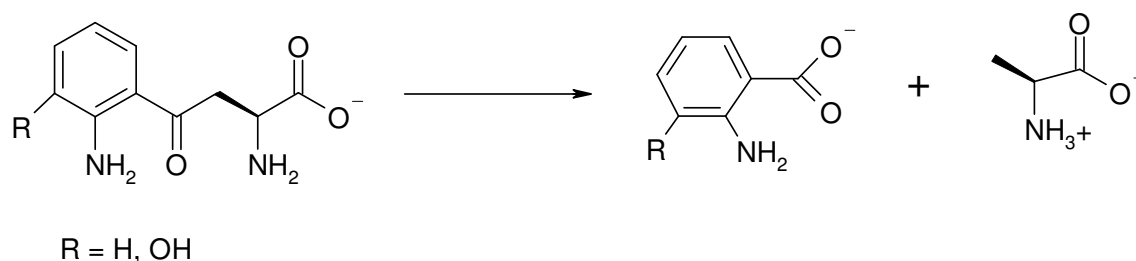
Scheme 3.1. Cleavage of kyn/3-hydroxy kyn by kynureninase.

3.3 Results and Discussion

Synthesis of 5. Compound **5** was designed as an analogue of 3-OH-Kyn that would bind to HKynase and be stable during cocrystallization for up to several weeks. The synthesis of **5** started from readily available 3-hydroxybenzaldehyde (**1**), (Scheme 3.2). After protection of the hydroxyl group in **5**, 3-hydroxyhippuric acid. **1** with ethylchloroformate to obtain 3-ethoxycarbonyloxybenzaldehyde (**2**), the aldehyde was oxidized to 3-ethoxycarbonyloxybenzoic acid (**3**) with oxone in DMF. The carboxylic acid

(**3**) was then converted to 3-ethoxycarbonyloxybenzoyl chloride (**4**) with oxalyl chloride. Finally, deprotection of the hydroxyl group of **4** and formation of **5** was achieved in a single step by the reaction of **4** with glycine in the presence of 0.5 M sodium hydroxide. The product **5** is at least 98% pure based on HPLC and 1H NMR.
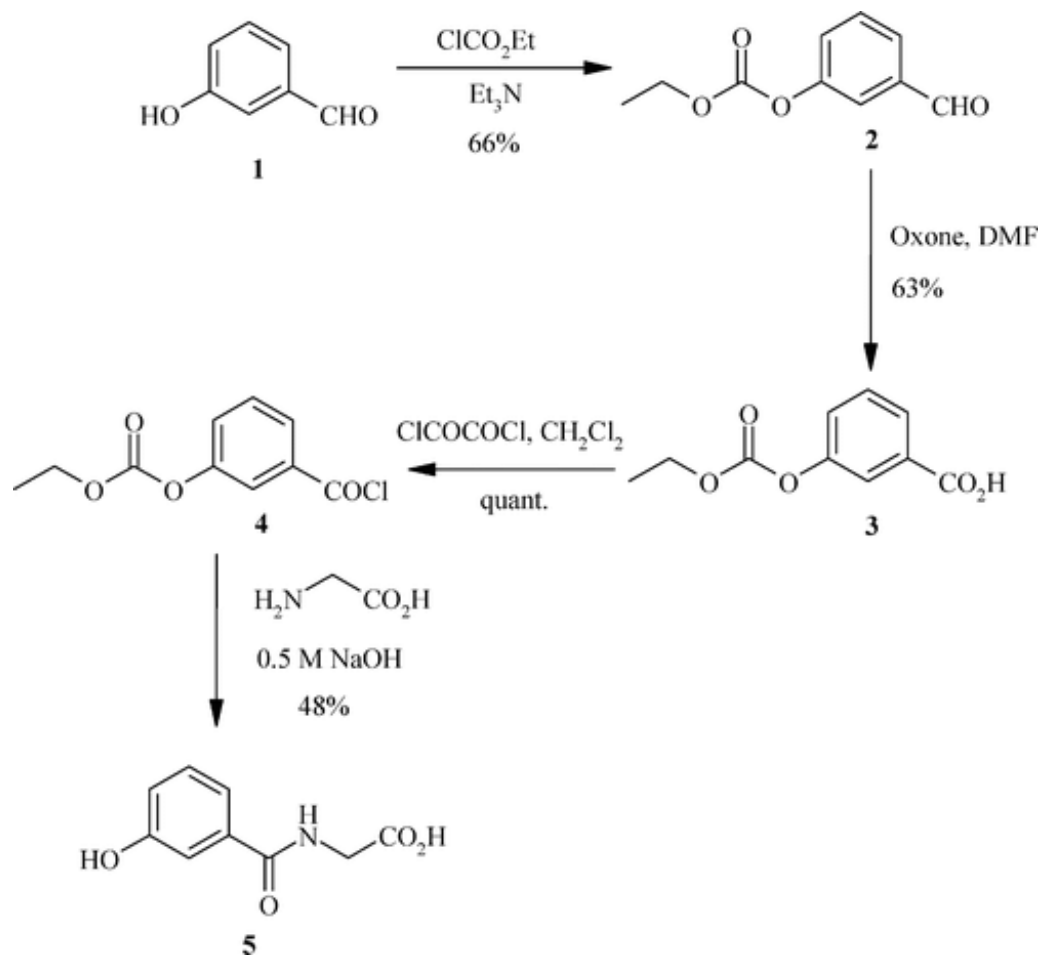
Scheme 3.2. Synthesis of 3-hydroxyhippuric acid

5
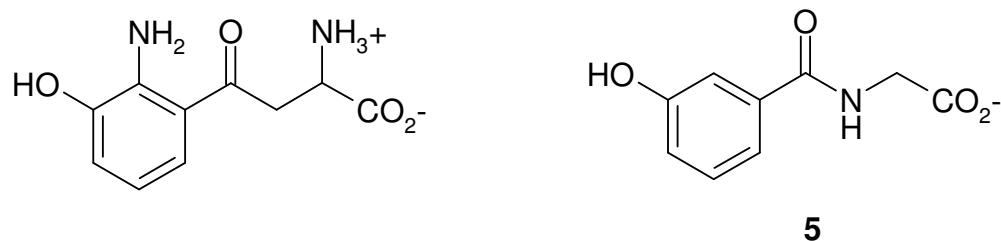
Scheme 3.3. Structural similarity between 3-OHkyn and 3-OH hippuric acid

Inhibition of Hkynase by 5. Our previous efforts to complex HKynase crystals with substrate and analogues had proven unsuccessful due to severe crystal cracking immediately upon exposure to the compounds in solution. Substituted hippurates were chosen for complexation because these compounds are structural analogues of L-Kyn/3-OH-Kyn (Scheme 3.2), which can form a Michaelis complex with HKynase. Because the hippurates do not have a free amino group, they bind without forming a covalent adduct with PLP, thus avoiding the structural rearrangements associated with substrate binding,[19] common among PLP-dependent aminotransferases, which can lead to crystal cracking during complexation. The parent compound, hippuric acid, does not show any detectable inhibition of HKynase at 1 mM. Of the other substituted hippurates tested, 2-amino-3-hydroxyhippuric acid (synthesis not shown) oxidizes rapidly in solution and thus could not be used in incubations to grow crystals. 2-aminohippuric acid proved to be unsuitable because it also did not inhibit HKynase at a concentration of 1mM. Compound **5** was the most stable inhibitor of the substituted hippurates tested and was thus chosen for the cocrystallization experiments. This compound was found to be a moderate competitive inhibitor of HKynase with a K_i of 60 μM. The fact that **5** is the most potent inhibitor of the compounds tested reflects the contribution of the 3-OH moiety to substrate specificity observed between kynurenine and 3-hydroxykynurenine

among kynureninases.[18] Inhibitors that contain an R-amino group capable of forming an external aldimine with the PLP do not require the 3-OH to bind to HKynase because compounds such as 2-ethoxybenzoylalanine[20] are also modest kynureninase inhibitors. However, the most potent inhibitor known for HKynase is 2-amino-4-[3′-hydroxyphenyl]-4-hydroxybutanoicacid, which contains both an R-amino group and the 3-OH, with a K_i value of 100nM.[21]**Human Kynureninase-5 Inhibitor Complex.** Statistics for the refined model are presented in Table 3.1.

Table 3.1 Summary of Crystallographic Analysis

Data collection & processing statistics		Refinement statistics	
space group	$C2$	R_{factor} (outer shell)	$0.154\ (0.251)^{b}$
resolution range(outer shell), Å	89.09-1.65 (1.68-1.65)	$R_{free}{}^{a}$ (outer shell)	0.190 (0.342)
no. of reflections (outer shell)	55449(2096)	mean B value, Å^2	16.65
average I /σI (outer shell)	24.1 (1.9)	rmsd from ideal geometry bond angles, deg bond distances, Å	
redundancy (outer shell)	3.5 9 (2.3)	Ramachandran plot residues in favored/allowed/disallowed regions. %	1.067
completeness (outer shell), %	96.3 (68.4)		0.007
R_{merge} (outer shell)	0.050 (0.362)		97.06/2.71/0.23

[a] R_{free} calculated with 5.1 % of the total data that were excluded from refinement.
[b] The outer shell resolution range used in refinement was 1.69-1.65 Å.

The structure (PDB accession number 3E9K) contained one monomer per asymmetric unit and had good geometry with 441/1 residues in the allowed/disallowed regions of the Ramachandran plot. The final model was refined to an R_{value} of 0.152, R_{free} value of 0.189, and covers 96% of the predicted amino acid sequence with 669 water molecules included in the final structure. The biologically active unit (dimer) can be generated by applying the crystallographic symmetry operator 1-x, -y, -z to the monomer. The regions between residues 1-5, 377-387, and 461-465 could not be modeled due to poorly ordered electron density. These regions had disordered electron density in the native HKynase structure as well.[18] Electron density could be seen extending between the ε amino group of Lys-276 and the C-4′ of PLP, an observation consistent with a PLP internal aldimine covalent adduct. Positive density for the **5** molecule could be clearly observed in a difference electron density map (Fo - Fc) calculated from the unrefined molecular replacement solution. Upon docking the molecule of **5**, electron density for the atoms improved and became continuous (Figure 3.1).
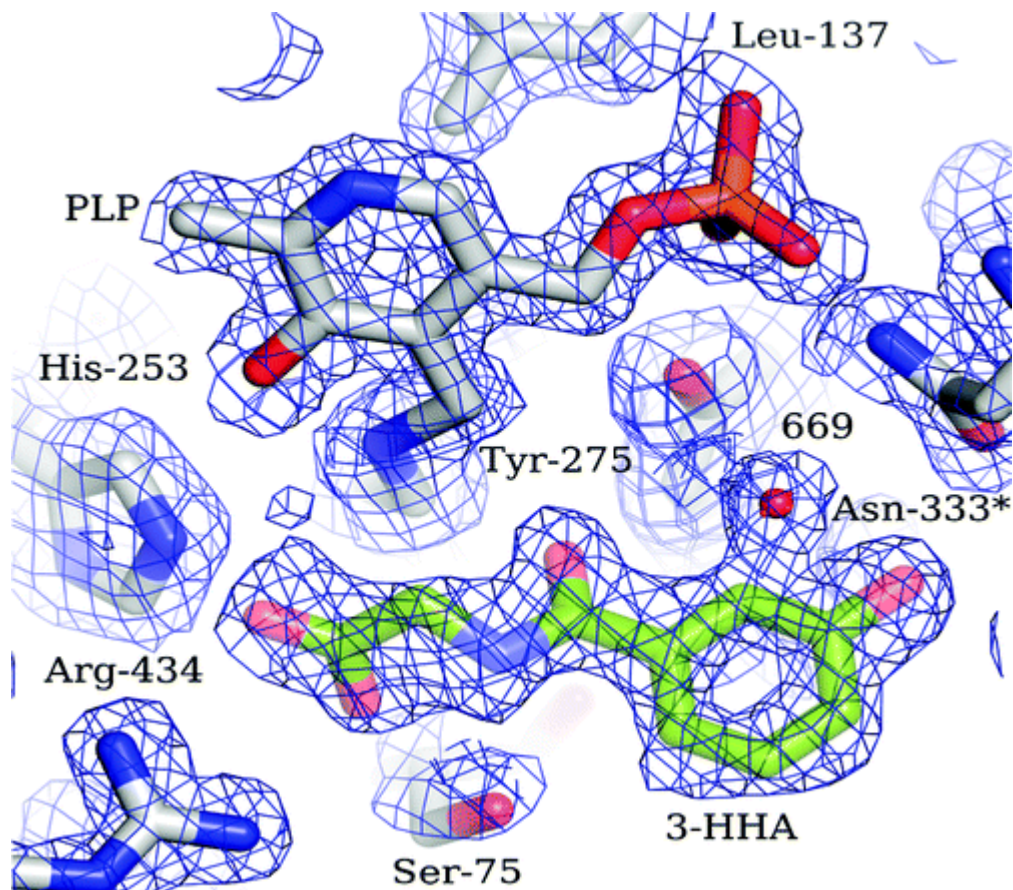
Figure 3.1 Electron density map showing continuous electron density for atoms of 5 (green carbon atoms, CPK coloring) in the active site of Hkynase.

Further refinement revealed the presence of two water molecules, water 669 and water 671, in difference electron density maps within a short distance of the C2 atom of the aromatic ring of **5**. Refinement of these waters and compound **5** at full occupancy produced density for both molecules at negative contour levels in a difference electron density map. Upon adjustment of occupancies to 20% for water 669 and 671 and 80% for compound **5**, no residual positive or negative density (<3σ) could be observed for either molecule. Interestingly, water 669 occupies a position relative to **5** similar to that which would be occupied by a substituent at the 2-position of the aromatic ring of **5**. Water 669 is stabilized by hydrogen bonds to the hydroxyl group of Tyr-275 (2.90 Å)

and the δ NH2 group of Asn-333* (3.19 Å) (*) denotes residues on the 2-fold symmetry related monomer). Thus, this partial occupancy water molecule reveals some of the interactions that are likely to stabilize the 2-amino substituent on the aromatic ring in 3-OH-Kyn and L-Kyn. The molecule of **5** is stabilized within the HKynase active site by interactions with residues from both monomer chains. The aromatic ring moiety of **5** lies in the active site pocket between the side chains of Ile-110*, His-102*, Tyr-275, Trp-305*, Phe-306*, Phe-314*, and Asn-333* (Figure 2). Trp-305* and Phe-314* stabilize **5** via alignment of their molecular quadrupole moments toward the aromatic ring (3.53 and 3.73 Å, respectively) and sandwich it with a π-stacking interaction against the side chain of His-102*. Trp-305 is strictly conserved in kynureninases of both eukaryotic and prokaryotic origin. Interestingly, Trp-305* also participates in cofactor binding by hydrogen bonding

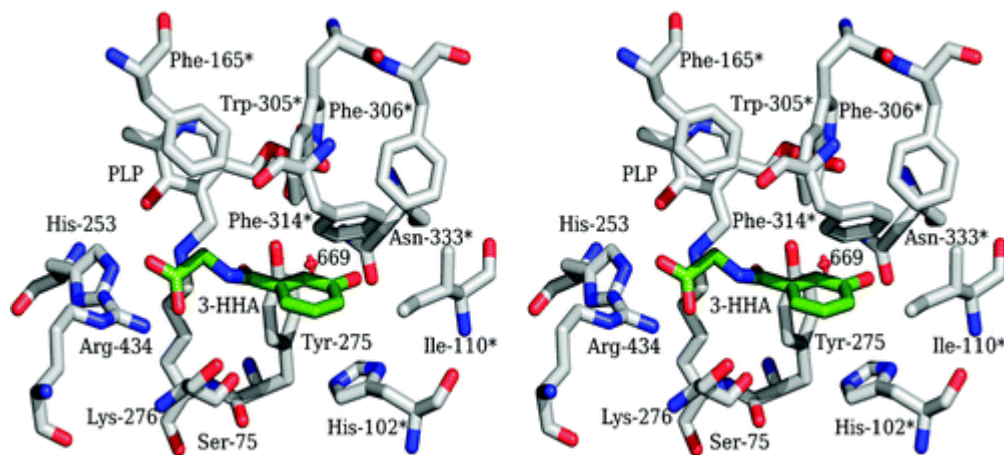**Figure 2. Relaxed-eye stereo representation of the binding interactions of 5 (colored green, ball and stick atoms) within the HKynase active site. Residues contributed from the symmetry related monomer are labeled with an asterisk (*).**

through its side chain pyrrole nitrogen with a PLP phosphate oxygen. Among PLP-dependent aminotransferases, the external aldimine scissile bond must be aligned

perpendicular to the plane of the cofactor ring system in order to minimize the energy of the upcoming transition state.[22] Thus, maintaining the appropriate geometry between cofactor and substrate in order to maximize σ-π overlap of the breaking bond with the cofactor π-system is crucial to catalysis. This complex reveals that Trp-305* likely plays a key role in maintaining the geometry of the external aldimine covalent adduct and subsequent intermediates by interacting with both substrate and cofactor. Moreover, Trp-305* is held firmly in position, relative to both cofactor and ligand, by two flanking quadrupole π-stacking interactions with the side chains of Phe-165 and Phe-306*. Phe-165 is a crucial active site residue because it participates in cofactor binding by π-stacking with the pyridine ring moiety of PLP. Phe-165 is stabilized in this position by one further quadrupole π-stacking interaction with the side chain of Phe-225. Phe-165, Trp-305*, and Phe-314* are strictly conserved among kynureninases regardless of their substrate specificity. Furthermore, all kynureninases have either a histidine or tryptophan residue at the bottom of the active site cavity to provide a π-stacking interaction to the substrate ring moiety. Other interactions that stabilize **5** in the HKynase active site include hydrogen bonding between the 3-hydroxyl ring substituent and the side chain δ oxygen of Asn-333* (3.54 Å). Also, the carbonyl oxygen of **5** is involved in a weak hydrogen bond with the hydroxyl oxygen of Tyr-275 (3.77 Å) and the amide nitrogen of **5** is within hydrogen bonding distance to the Ser-75 γ oxygen (3.63 Å). On the other side of the active site cavity, and near the Lys-276-PLP internal aldimine imine bond, the carboxylate of **5** forms an ion pair with Arg-434 (2.98 and 3.06 Å), and hydrogen bonds with the ε nitrogen of His-253 (2.74 Å), and with the γ oxygen of Ser-75 (2.88 Å). The interaction between the carboxylate of **5** (which is equivalent to

the R-carboxylate of L-enantiomer substrates) with the strictly conserved Arg-434 is well characterized among members of the PLP-dependent aspartate aminotransferase superfamily and is crucial to catalysis.[19,23,24] A structural superposition of native (PDB accession code 2HZP) and **5** complexed HKynase reveals no major structural conformational changes. However, the side chains of residues Tyr-226, Arg-428, and Arg-434 showed conformational differences associated with the presence of **5**. Specifically, Arg-434 forms an electrostatic bond with the carboxylate oxygens of **5**. To do so, the Arg-434 guanidino nitrogens must move 7.7 Å from the position observed in native HKynase.[18] Consistent with the partial occupancy for **5**, the difference electron density map suggests two conformational states for the side chain of Arg- 434: a high occupancy state (80%) in which the side chain interacts with the carboxylate oxygens of **5**, and a low occupancy state (20%) in which no ligand is present in the active site and the Arg-434 side chain conformation resembles that of native. HKynase. Similarly, Tyr-226 and Arg-428 showed additional density in a difference electron density map, suggesting that these residues must adopt different conformations in order to accommodate **5** in the active site cavity. These residues were modeled to have 80% and 20% conformations as well. Interestingly, these residues do not directly contact ligand atoms, yet they line the surface of an interdomain channel that leads to the active site cavity. Thus, these residues appear to be dynamically involved in substrate binding by allowing access to the active site. The position of the side chains of these residues in ligand bound kynureninase places them at 4.4 Å (between hydroxyl oxygens of Tyr-226) and 3.7 Å (between guanidine nitrogens of Arg-428) from those in native HKynase. The structure of the HKynase-**5** complex provides new insights into the catalytic mechanism

of kynureninase. In previous studies on the mechanism of kynureninase from *Pseudomonas fluorescens*, we determined the stereochemistry of inhibition by transition state analogues and proposed that a general acid-base catalyst was involved in hydration of the substrate carbonyl and cleavage of the resulting *gem*-diol to give the carboxylic acid product.25 The stereochemistry of inhibition by dihydrokynurenine and retro-aldol reactions catalyzed by kynureninase suggested that the water addition occurred from the *re*-face of the carbonyl.[25] In the present structure, the face of the inhibitor carbonyl equivalent to the *re*-face of the substrate is exposed, and the opposite face is covered by the ring of Tyr- 275 and the side chain of Ser-75. Thus, the structure of the 5-HKynase complex is consistent with the stereochemistry of inhibition by dihydrokynurenine and suggests Tyr-275 may be an auxiliary acid-base catalyst for the reaction. Supporting the idea that Tyr-275 may play a critical role in catalysis is the observation that this Tyr residue is strictly conserved in all known kynureninase sequences (Figure 3.1). In addition, Ser-75 could potentially donate a hydrogen bond to the carbonyl, and it is also strictly conserved (Figure 3.3). A plausible mechanism for HKynase, taking into account the new structural data, is shown in Scheme 3.4. In the 3-OH-Kyn Schiff's base, Lys-276 removes the R-proton to form a quinonoid species, which is rapidly reprotonated at C-4′ to form a ketimine.26 Lys-276 can then act as a general base to deprotonate a water molecule so that it can add to the carbonyl. A potential donor for the *gem*diol of the reaction intermediate is water-657 hydrogen bonded to the side chain of Asp-426. We note that **5** is not quite positioned like a substrate would be because the R-hydrogen would have to be closer to Lys-276 for proton abstraction. The reaction of substrate with the PLP would likely result in

reorganization of the active site bringing the catalytic residues into position. Interestingly, the complex shows that Tyr-275 also hydrogen bonds with the PLP phosphate, which suggests a possible involvement of its side chain in the catalytic cycle by mediating a proton transfer from the phosphate to the carbonyl.
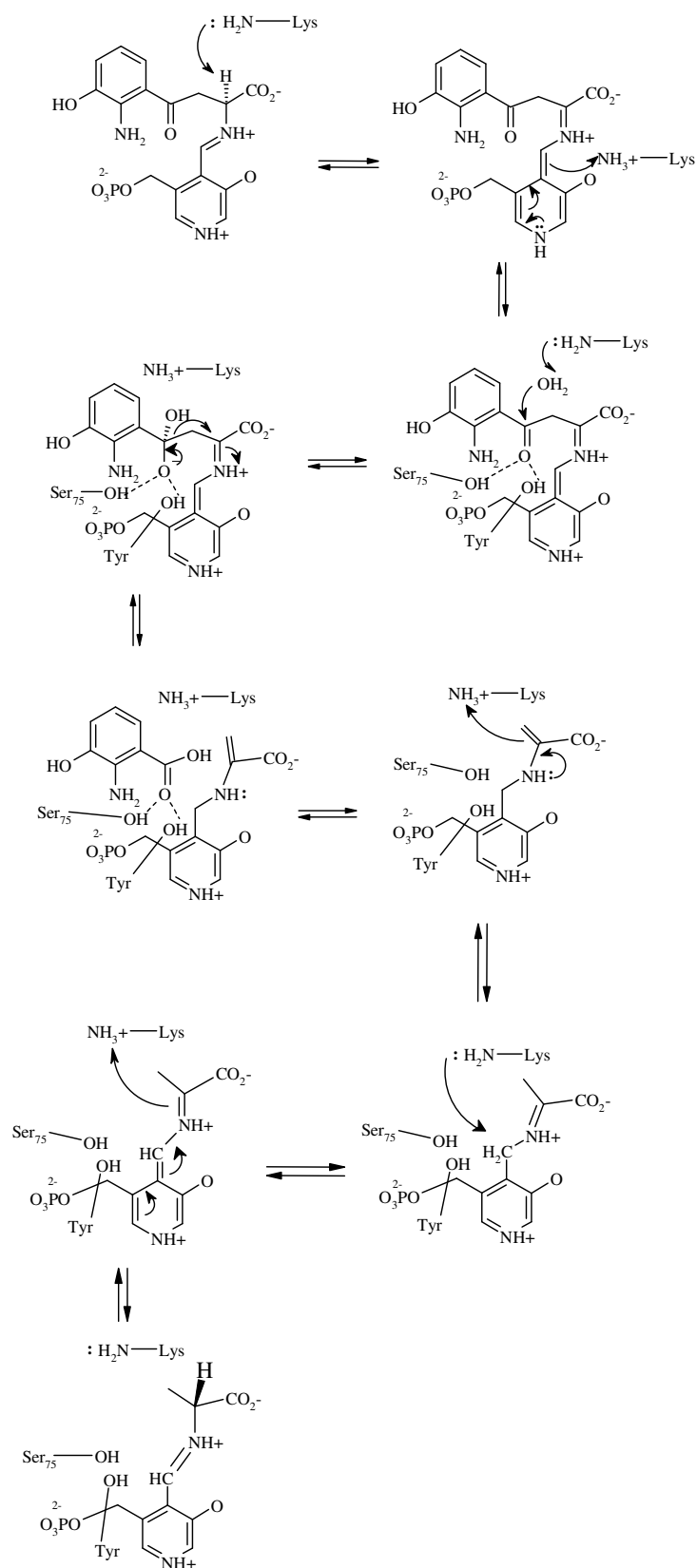
Scheme 3.4. Mechanism for the reaction Hkynase with its natural substrate

In this scenario, Tyr-275 could initiate C_γ-C_β cleavage by deprotonation after formation of the *gem*-diol intermediate. The proposed mechanistic model resembles that of tyrosine phenollyase, where we found that Tyr-71 forms a hydrogen bond with the PLP phosphate in the internal aldimine and donates a proton to the phenol leaving group during catalysis.[27]

Kinetic Characterization of HKynase Mutants.

The structure of **5** bound in the active site, shown in Figure 3.2, shows that Asn-333* accepts a hydrogen bond from the 3-OH of the bound ligand. As shown in the sequence alignments in Figure 3.1, the corresponding residue in bacterial kynureninase is a Thr. Characterization of the kinetic properties of the HKynase N333T mutant revealed a 9-fold decrease in k_{cat} for L-Kyn, but no change in K_m (Table 2). This mutant has weaker 3-OH-Kyn binding (6-fold higher K_m) and k_{cat} at least 1100 times slower than wild type HKynase. Thus, this mutation affects 3-OH-Kyn binding and reduces its catalytic efficiency (k_{cat}/K_m) by a factor of more than 6 × 103, whereas the k_{cat}/K_m for L-Kyn is reduced only 9-fold. Hence, the hydrogen bond formed between the 3-OH group in 3-OH-Kyn and the carbonyl oxygen of Asn-333* appears to be an important determinant for the 3-OHKyn reaction. It is important to note that the K_m and V_{max} values of 3-OH-Kyn for N333T and S332G/N333T mutants could not be accurately determined, as rates for high concentrations of 3-OH-Kyn showed significant substrate inhibition. Thus, K_m values for N333T and S332G/N333T HKynase are estimated as greater than the highest 3-OH-Kyn concentration at which hydrolysis rates were still increasing in a linear fashion. The k_{cat}/K_m values for these mutants were calculated from the second order rate constant obtained from the linear portion of a V vs [S] plot. Subsequently, the

estimated K_m and calculated k_{cat}/K_m values were used to estimate the upper limit of k_{cat}. N333T and S332G/N333T mutant HKynases show a very slight preference for L-Kyn over 3-OH-Kyn (Table 3.2). Isolation and characterization of H102W mutant HKynase was not possible because it could not be purified from the soluble cellular extract and appeared entirely in the insoluble protein fraction. We did not attempt to solubilize and refold protein from the inclusion bodies that resulted from these cultures. This protein in the insoluble pellet was of identical apparent SDS-PAGE molecular weight as wild-type HKynase. However, combination of the H102W and N333T mutations in the H102W/N333T double mutant restored the expression of soluble protein to levels similar to that of wild-type HKynase. These results are consistent with the observation that kynureninases contain pairings of residues at these positions that are consistently either His/Asn or Trp/Thr, as can be seen in Figure 3. Characterization of the HKynase mutant H102W/N333T revealed a small decrease in k_{cat} and K_m values for L-Kyn so that the k_{cat}/K_m value only decreases about 2.5-fold. However, the H102W/N333T mutant HKynase did not exhibit any measurable activity with 600 μM 3-OH-Kyn and 37.2 μM HKynase. Thus, these values were used to estimate a theoretical upper limit for k_{cat}/K_m by assuming 3-OH-Kyn $K_m \geq 600$ μM and $V_{max} \leq 0.0001$ absorbance min^{-1}, the minimal rate that could be measured. The net effect of the H102W/N333T double

mutation is a decrease in catalytic efficiency toward 3-OH-Kyn by a factor of at least 7.5 × 106 when compared to that of wildtype HKynase.

Table 3.2 L-Kynurenine and 3-OH-DL-Kynurenine Kinetic Constants for Wild-Type and Mutant HKynases

Enzyme	L-Kynurenine			3-OH-DL-Kynurenine			L-Kyn /3-OH-DL-Kyn
	K_m (μM)	k_{cat} (s^{-1})	k_{cat}/K_m (M^{-1} s^{-1})	K_m (μM)	k_{cat} (s^{-1})	k_{cat}/K_m (M^{-1} s^{-1})	k_{cat}/K_m ratio
wild type	495	0.230	465	28.3	3.5	1.23×10^5	3.78×10^{-3}
N333T	499	0.026	52.1	>200	$< 3.9 \times 10^{-3}$	19.8	2.6
S332G/N333T	540	0.017	31.4	>510	$< 10.9 \times 10^{-3}$	21.5	1.5
H102W/N333T	327	0.007	21.4	N/A	N/A	<0.0165	$>1.36 \times 10^3$
H102W/S332G/N333T		0.018	125.6	N/A	N/A	<0.0165	$>7.61 \times 10^3$

Thus, removing the hydrogen bonding partner at the δ-position of Asn-333, increasing the local nonpolar environment, and introducing a large bulky side chain (Trp) at position 102 effectively act to exclude any 3-OH-Kyn binding at the concentrations measured. This suggests that residues Asn-333 and His-102 are the primary substrate specificity contacts for the 3-substituent on the kynurenine aromatic ring. Although the overall ratio of substrate specificity for 3-OH-Kyn/L-Kyn is reversed in the H102W/N333T mutant, this mutant is 22-fold less efficient at hydrolyzing L-Kyn than the wild-type enzyme. This suggests that a surrounding shell of residues contribute to catalytic efficiency. To further probe which residues contribute to catalytic efficiency, we introduced a third mutation, S332G, a residue showing a conserved pattern among orthologues utilizing L-Kyn or 3-OH-Kyn similar to that of His-102 and Asn-333 (Figure 3.3). In most 3-OH-Kyn hydrolyzing kynureninases, a Ser residue is conserved at this position, whereas the enzymes from organisms lacking the 3-OH-Kyn metabolite contain a conserved Gly (Figure 3.3). In the HKynase-**5** complex, Ser-332 does not form hydrogen bonds or have electrostatic contacts with any atoms of **5**. Yet, Ser-332 forms a hydrogen bond through the backbone amide nitrogen with one of the PLP phosphate oxygens. Characterization of the H102W/S332G/N333T triple mutant showed it has the strongest activity and catalytic efficiency toward L-Kyn of all Hkynase mutants studied. Furthermore, it showed no detectable activity with 3-OH-Kyn (Table 3.2) and has a 6-fold improvement in k_{cat}/K_m over the H102W/N333T mutant Hkynase. Thus, this mutation restores catalytic efficiency with L-Kyn to one-third of that measured with wild-type enzyme.

```
Bacillus          IYLDGNSLGL GIDGWTEGE. NYKYLNAGPG AYQIGTPHVL
Clostridium       IYMDGNSLGL AIKIWGVED. SYKYLNGGPG GFLLGTHNMF
Pichia            IYLCGNSLGL GVESHFNHPG SYKYLNSGPG SYRQSNPSVI
Saccharomyces     TYLCGNSLGL AVESHFKHPE SYKYLNAGPG GFRQSNPSVI
Aspergillus       LYLCGNSLGL GVTGHFVQHD TYKYLNSGPG GFQLSNPSVL
Shewanella        LYFTGNSLGL GVEGHFHAV. TYKYLNSSAG GWQISNAPVM
Cytophaga         AYFCGHSLGL GVEGHWKAA. SYKYLNGGPG GFQVSNAPVF
Myxococcus        VYLAGNSLGL GVEGHHHGR. SYKYLNAGPG GWQLSNPPIF
Stigmatella       VYLAGNSLGL GVEGHFHAR. SYKYLNGGPG GWQLSNPPIF
Acidobacteria     VYLVGHSLGL GVEGHFRGK. SYKYLNGGPG GWQLSNPSIL
Xanthomonas       TYLVGNSLGL GVEGHFTGP. NYKYLNAGPG GWQLSNPPVL
Human             IYFLGNSLGL AAYGHEVGK. SYKYLNAGAG GFRISNPPIL
Dog               IYFSGNSLGL GVYGHEVGK. SYKYLNSGAG GFRISNPPIL
Rat               IYFLGNSLGL GAYGHEVGK. SYKYLNSGAG GFRISNPPIL
Mouse             IYFLGNSLGL GAYGHDVGK. SYKYLNSGAG GFRISNPPIL
Chicken           IYFVGNSLGL GVHGHFNGQ. TYKYLNSGAG GFRLSNPPIL
Zebra fish        IYFAGNSLGL GVHGHTEGS. TYKYMNSGAG GFRLSNQPIL
Caenorhabditis    IYLCGNSLGL GVFGHMSGE. SYKYGCTGAG GYRISNPPIH
Dictyostelium     IYLTGNSLGL GVEGHHKGD. TYKYLNSGPG GFRMSNPSVA
Pseudomonas       IYLDGNSLGA LIRSWNTAG. TYKYLNGGPG RYLCGTQPIT
Burkholderia      IYLDGNSLGA LIRSWNTAG. TYKYLNGGPG RFLCGTQPIV
Comamonas         IYLDGNSLGA LITSWNKAG. SYKYLNGGPG RYLCGTQPMI
Ralstonia         IYLDGNSLGA LIRSWNDAD. GYKYLNGGPG RMLTGTAPQL
Oceanicola        VYMDGNSLGP LITAWNRAG. SYKFLNGGPG RMRVGTPPMI
Rhodobacter       IYLDGNSLGP LITGWNRAG. TYKYLNSGPG RMRVGTPPVI
Bradyrhizobium    IYLDGNSLGA LIRGWNSAG. TYKYLNGGPG RMRIGTPPII
Silicibacter      IYLDGNSLGP LIKAWNTAD. TYKYFNGGPG RLRVGTPSIV
Erythrobacter     IYLDGNSLGC LIRSWNEAG. GYKYLCGGPG QLQCGTSPVL
Arthrobacter      SYLDGNSLGR LIRGWD.EE. TYKYLNGGPG GFLSGTPAIF
                  69       78 98       106 274     283 328    337
```

Figure 3.3. Sequence alignments of kynureninases from various organisms. Numbers at the bottom refers to the human sequence.

In contrast, the S332G/ N333T double mutant shows no improvement in k_{cat}/K_m over that measured in the N333T single mutant. From these results, we infer that the increased backbone flexibility provided by Gly-332 facilitates the interaction between Thr-333 and the bulky side chain of Trp-102, allowing a better fit of L-Kyn within the mutant active site cavity. This result suggests that two shells of residues surrounding the ligand atoms determine catalytic efficiency in kynureninases. One shell of residues directly contacts ligand atoms, providing essential acid/base, steric, and electrostatic interactions, and the other contributes remotely to the geometric arrangement of the active site and plays a dynamic role in catalysis. Interestingly, kynureninase from

Ralstonia metallodurans was reported to have comparable activity with both L-Kyn and 3-OH-Kyn.[28] Yet, as shown in Figure 3.3, this kynureninase has an active site that contains the Trp/Gly/Thr pairing, further emphasizing the role played by outer shell residues in substrate specificity and catalysis. It will be of interest to use the HKynase H102W/S332G/N333T triple mutant for directed evolution experiments to identify residues remote from the active site which contribute to specificity and catalysis. Currently, a number of kynureninase inhibitors have been reported in the literature.[20,21,25,29-33] Until now, their design has been based primarily on mechanistic considerations due to a lack of knowledge regarding the primary substrate binding mode and substrate-enzyme interactions required for in silico directed drug design. The HKynase-**5** complex reveals important restraints for the design and screening of novel substrate analogues and inhibitors. First, the following atoms should be designated as potential hydrogen bonding partners for ligand atoms: the side chain δ-oxygen of Asn-333*, the side chain hydroxyl oxygen of Tyr-275, and the γ-oxygen of Ser-75.Second, hydrophobic interactions should be maintained between aromatic substituents on screened ligands and the side chains of Ile-110*, Trp-305*, Phe-306*, and Phe-314*. HKynase-**5** interactions clearly show that a strong quadrupole molecular alignment occurs between the side chains of Trp-305*, Phe-314*, and the aromatic ring moiety of **5**, as well as ligand π-stacking against the side chain of His-102*. Third, electrostatic and/or hydrogen bonding interactions should be assigned between ligand atoms and the guanidino nitrogens of Arg-434 and the imidazole nitrogen atoms of His-253. Fourth, our results clearly show that His-102 and Asn-333 are the residues involved in substrate specificity for 3-OH-Kyn. As such, the interaction between these residues and ligand

atoms should be used as a one of the primary forms of binding mode evaluation in docking studies. Furthermore, scoring of docked poses should consider the interaction between ligand atoms and Arg-434 side chain atoms as a strong indicator of acceptable docking because this form of stabilization is known to be crucial in ligand binding and stabilization throughout the PLP-dependent aspartate aminotransferase family of enzymes. Finally, we note that **5** is an ideal lead compound for combinatorial synthesis of libraries of possible HKynase inhibitors.

3.4 Experimental Section

Crystallization, Data Collection, and Molecular Replacement.

Human kynureninase was expressed and purified as previously described.[18] Complexed kynureninase-3-hydroxyhippuric acid crystals were grown using the modified microbatch under oil technique at 25°C by mixing (1:1 ratio) an HKynase solution (9 mg ml-1 in 50 mM HEPES, pH 5.1, and 0.1 mM PLP) with a crystallization solution containing 0.05 M $MgCl_2$, 0.1 M Tris (pH 8.0), 25% PEG 3000 and 350 μM **5**. Dark-yellow crystals appeared after 4-5 weeks and grew to dimensions of 0.075 mm × 0.05 mm × 0.015 mm. These crystals were flash frozen in liquid nitrogen with cryoprotectant containing 1 mM **5**, 55 mM $MgCl_2$, 110 mM Tris (pH 8), 33% PEG 3000. These crystals had space group *C*2 with cell constants a = 74.44 Å, b = 77.12 Å, c = 94.55 Å, β = 109.35. X-ray synchrotron data were collected (λ) 1.007 Å, 200 frames, 1° oscillations) at the Advanced Photon Source beamline 19-ID and were processed and scaled with HKL3000.[34] The merged SCALEPACK[34] intensities were used as input for the molecular replacement program Phaser[35] using the HKynase (PDB accession code 2HZP) (HKynase) coordinates as

the phasing model. All water, hetero, and PLP coordinates were deleted from the input model. The molecular replacement solution and Hkynase-**5** complex were refined with Refmac5.[36] Water addition was done with ARP/ wARP.[37] The PLP cofactor and compound **5** were manually

introduced with COOT.[38] TLS[39] refinement was performed with the following groups: 6-37, 38-45, 46-120, 121-190, 191-213, 214-357, 358-375, 376-412, 413-460. The model of **5** and library description were created with the CCP4i Monomer Library Sketcher.[40] Molprobity[41] was used to evaluate the quality of the final model.

Inhibition Kinetics. Compound **5** was evaluated for its ability to inhibit the reaction of HKynase with its cognate substrate, 3-OHKyn. Assays were performed by following the absorbance change at 370 nm as 3-OH-Kyn (DL mixture, USBiochemical Corp.) is converted to 3-hydroxyanthranilic acid and L-Alanine ($\Delta\varepsilon$)-4500 M-1 cm-1) with a Cary 1 UV/visible spectrophotometer equipped with a Peltier temperature controlled cell 6 × 6 cell compartment. Assays contained 30 mM potassium phosphate, pH 8.0, and 40 μM PLP at 37 ℃ together with variable amounts of 3-OH-Kyn and four different concentrations of **5**. Data were fit to a competitive inhibition model with Cleland's COMPO program.[42]

Site Directed Mutagenesis. Mutants were created using the QuickChange site-directed mutagenesis kit (Stratagene). The following mutants were created and sequenced to confirm the desired codon change: H102W, N333T, S332G/N333T (double mutant), H102W/N333T (double mutant), H102W/S332G/N333T (triple mutant). The mutagenesis primers used were (only coding strand written, mutated bases bold underlined): H102W: 5′-CCA AAA TAG CAG CCT ATG GT**T GG**G AAG

TGG GGA AGC GTC CTT GG-3′; S332G/N333T: 5′-GGG GTC TGT GGA TTC CGA

ATT **GGC** A**CC** CCT CCC ATT TTG TTG GTC-3′; N333T: 5′-

GTC TGT GGA TTC CGA ATT TCA A**CC** CCT CCC ATT TTG TTG G-3′.

Synthesis of 3-Hydroxyhippuric Acid (5).

3-Ethoxycarbonyloxybenzaldehyde (2).[43]

3-Hydroxybenzaldehyde (1; 15.0 g, 0.123 mol) was dissolved in 100 ml dry pyridine,

cooled to 4 °C, and ethyl chloroformate (20 ml) was added dropwise over a period of 30

min. The resulting solution was stirred for 2 h at room temperature. The solvent was

evaporated in vacuo, and water (150 ml) was added to the residue. The product was

extracted into ether, and the extract was washed consecutively with water, 5% HC1, 5%

cold NaOH, and again with water. The dried organic extract was evaporated in vacuo to

give a dark-red viscous product (15.5 g, 65%). 1H NMR (400 MHz, CDCl3) δ 1.29 (t,

3H), 4.21 (m, 2H), 7.96 (dd, 1H), 7.57 (d, 1H), 7.72 (d, 1H), 7.74 (m, 1H), 9.61 (s, 1H).

3-Ethoxycarbonyloxybenzoic acid (3).[44] 3-Ethoxycarbonyloxybenzaldehyde

(6 g, 0.03 mol) was dissolved in 30 ml DMF. Oxone (19 g, 0.03 mol) was added, and the

mixture was stirred at room temperature for 3 h. The reaction was monitored by TLC

and, after completion, 1 N HCl was added to dissolve the salts. The crude product was

extracted into ethyl acetate (50 ml), the organic extract washed with 1N HCl (3 × 15 ml),

brine (2 × 10 ml), and then dried over Na_2SO_4. Evaporation of the solvent in vacuo gave

3-ethoxycarbonyloxybenzoic acid (**3**), which was purified by silica gel column

chromatography (60:40 EtOAc/hexane). Yield, 3.86 g (63%). 1H NMR (400 MHz,

CDCl3) δ 1.29 (t, 3H), 4.21 (m, 2H), 7.93 (dd, 1H), 7.63 (d, 1H), 8.02 (d, 1H), 8.06 (m,

1H), 12.54 (s,1H).

3-Ethoxycarbonyloxybenzoyl chloride (4). To 3.0 g (0.15 mol) of 3-ethoxycarbonyloxybenzoic acid in dry dichloromethane, one equiv of 0.2 M oxalyl chloride in dichloromethane was added dropwise, and the mixture was stirred for 5 h at room temperature. The crude 3-methoxycarbonyloxybenzoyl chloride (2.35 g, 68%) was obtained after evaporation of excess solvent and reagent. 1H NMR(400 MHz, CDCl3) δ 1.29 (t, 3H), 4.21 (m, 2H), 7.93 (dd, 1H), 7.66 (d, 1H), 7.96 (d, 1H), 8.00 (m, 1H).

3-Hydroxyhippuric acid (5).[45] The finely powdered 3-ethoxycarbonyloxybenzoyl chloride (1.7 g, 0.007 mol) was added to 0.6 g of glycine in 20 ml of 0.5 N NaOH. Subsequently, 1N NaOH was continuously added to the solution over a period of 15 min to maintain the pH above 10. The reaction mixture was then acidified with conc. HCl, and **5** was extracted with ethyl acetate (3 × 15 ml). The organic extracts were dried and evaporated, and the crude product was recrystallized from 50% ethanol-water. Yield, 0.8 g (48.3%), mp 184-187 °C. 1H NMR (DMSO-$d6$) δ 3.87 (d, 2H,CH2), 6.88-6.91 (m, 3H, Ar-H), 7.21-7.25 (m, 1H, Ar-H), 8.68(t, 1H, NH), 9.60 (s, 1H, OH), 12.60 (s, 1H, CO2H). MS, anion mode, direct injection ESI (M - H)-) 194.0 (100%); (2M -H)-) 389.2 (36%).

3.5 References

1. Soda, K.; Tanizawa, K. Kynureninases: enzymological properties and regulation mechanism. *AdV. Enzymol. Relat. Area Mol. Biol.* **1979**, *49*, 1–40.

2. Colabroy, K. L.; Begley, T. P. The pyridine ring of NAD is formed by a nonenzymatic pericyclic reaction. *J. Am. Chem. Soc.* **2005**, *127*, 840–841.

3. Schwarcz, R.; Whetsell, W. O., Jr.; Mangano, R. M. Quinolinic acid: an endogenous metabolite that produces axon-sparing lesions in rat brain. *Science* **1983**, *219*, 316–318.

4. Stone, T. W.; Perkins, M. N. Quinolinic acid: a potent endogenous excitant at amino acid receptors in CNS. *Eur. J. Pharmacol.* **1981**, *72*, 411–412.

5. Heyes, M. P.; Brew, B.; Martin, A.; Markey, S. P.; Price, R. W.; Bhalla, R. B.; Salazar, A. Cerebrospinal fluid quinolinic acid concentrations are increased in acquired immune deficiency syndrome. *AdV. Exp. Med. Biol.* **1991**, *294*, 687–690.

6. Achim, C. L.; Heyes, M. P.; Wiley, C. A. Quantitation of human immunodeficiency virus, immune activation factors, and quinolinic acid in AIDS brains. *J. Clin. InVest.* **1993**, *91*, 2769–2775.

7. Heyes, M. P.; Swartz, K. J.; Markey, S. P.; Beal, M. F. Regional brain and cerebrospinal fluid quinolinic acid concentrations in Huntington's disease. *Neurosci. Lett.* **1991**, *122*, 265–269.

8. Giorgini, F.; Moller, T.; Kwan, W.; Zwilling, D.; Wacker, J. L.; Hong, S.; Tsai, L. C.; Cheah, C. S.; Schwarcz, R.; Guidetti, P.; Muchowski, P. J. Histone deacetylase inhibition modulates kynurenine pathway activation in yeast, microglia, and mice expressing a mutant huntingtin fragment. *J. Biol. Chem.* **2008**, *283*, 7390–7400.

9. Guillemin, G. J.; Meininger, V.; Brew, B. J. Implications for the kynurenine pathway and quinolinic acid in amyotrophic lateral sclerosis. *Neurodegener. Dis.* **2005**, *2*, 166–176.

10. Leonard, B. E. Inflammation, depression and dementia: are they connected. *Neurochem. Res.* **2007**, *32*, 1749–1756.

11. Guillemin, G. J.; Brew, B. J.; Noonan, C. E.; Takikawa, O.; Cullen, K. M. Indoleamine 2,3 dioxygenase and quinolinic acid immunoreactivity in Alzheimer's disease hippocampus. *Neuropathol. Appl. Neurobiol.* **2005**, *31*, 395–404.

12. Stone, T. W.; Mackay, G. M.; Forrest, C. M.; Clark, C. J.; Darlington, L. G. Tryptophan metabolites and brain disorders. *Clin. Chem. Lab. Med.* **2003**, *41*, 852–859.

13. Schwarcz, R.; Pellicciari, R. Manipulation of brain kynurenines: glial targets, neuronal effects, and clinical opportunities. *J. Pharmacol. Exp. Ther.* **2002**, *303*, 1–10.

14. Stone, T. W.; Addae, J. I. The pharmacological manipulation of glutamate receptors and neuroprotection. *Eur. J. Pharmacol.* **2002**, *447*, 285–296.

15. Tankiewicz, A.; Pawlak, D.; Buczko, W. Enzymes of the kynurenine pathway. *Postepy. Hig. Med. Dosw.* **2001**, *55*, 715–731.

16. Shetty, A. S.; Gaertner, F. H. Kynureninase-Type enzymes of *Penicillum roqueforti*, *Aspergillus niger*, *Rhizopus stolonifer*, and *Pseudomonas fluorescens*: further evidence for distinct kynureninase and hydroxykynureninase activities. *J. Bacteriol.* **1975**, *122*, 235–244.

17. Toma, S.; Nakamura, M.; Tone, S.; Okuno, E.; Kido, R.; Breton, J.; Avanzi, N.; Cozzi, L.; Speciale, C.; Mostardini, M.; Gatti, S.; Benatti, L. Cloning and recombinant expression of rat and human kynureninase. *FEBS Lett.* **1997**, *408*, 5–10.

18. Lima, S.; Khristoforov, R.; Momany, C.; Phillips, R. S. Crystal structure of *Homo sapiens* kynureninase. *Biochemistry* **2007**, *46*, 2735–2744.

19. Jager, J.; Moser, M.; Sauder, U.; Jansonius, J. N. Crystal structures of *Escherichia coli* aspartate aminotransferase in two conformations. Comparison of an unliganded open and two liganded closed forms. *J. Mol. Biol.* **1994**, *239*, 285–305.

20. Chiarugi, A.; Carpenedo, R.; Molina, M. T.; Mattoli, L.; Pellicciari, R.; Moroni, F. Comparison of the neurochemical and behavioral effects resulting from the inhibition of kynurenine hydroxylase and/or kynureninase. *J. Neurochem.* **1995**, *65*, 1176–1183.

21. Walsh, H. A.; Leslie, P. L.; O'Shea, K. C.; Botting, N. P. 2-Amino-4-[3′-hydroxyphenyl]-4-hydroxybutanoic acid; a potent inhibitor of rat

and recombinant human kynureninase. *Bioorg. Med. Chem. Lett.* **2002**, *12*, 361–363.

22. Dunathan, H. C. Conformation and reaction specificity in pyridoxal phosphate enzymes. *Proc. Natl. Acad. Sci. U.S.A.* **1966**, *55*, 712–716.

23. Delle Fratte, S.; Iurescia, S.; Angelaccio, S.; Bossa, F.; Schirch, V. The function of arginine 363 as the substrate carboxyl-binding site in *Escherichia coli* serine hydroxymethyltransferase. *Eur. J. Biochem.* **1994**, *225*, 395–401.

24. Almo, S. C.; Smith, D. L.; Danishefsky, A. T.; Ringe, D. The structural basis for the altered substrate specificity of the R292D active site mutant of aspartate aminotransferase from E. coli. *Protein Eng.* **1994**, *7*, 405–412.

HKynase-3-Hydroxyhippuric Acid Inhibitor Complex Journal of Medicinal Chemistry, 2009, Vol. 52, No. 2 **395**

25. Dua, R.; Phillips, R. S. Stereochemistry and mechanism of aldol reactions catalyzed by kynureninase. *J. Am. Chem. Soc.* **1991**, *113*, 7385–7388.

26. Phillips, R. S.; Sundararaju, B.; Koushik, S. V. The Catalytic Mechanism of Kynureninase from *Pseudomonas fluorescens*: Evidence for Transient Quinonoid and Ketimine Intermediates from Rapidscanning Stopped-flow Spectrophotometry. *Biochemistry* **1998**, *37*, 8783–8789.

27. Chen, H. Y.; Demidkina, T. V.; Phillips, R. S. Site-directed Mutagenesis

of Tyrosine-71 to Phenylalanine in *Citrobacter freundii* Tyrosine

Phenol-lyase: Evidence for Dual Roles of Tyrosine 71 as a General

Acid Catalyst in the Reaction Mechanism and in Cofactor Binding.

Biochemistry **1995**, *34*, 12276–12283.

28. Kurnasov, O.; Goral, V.; Colabroy, K.; Gerdes, S.; Anantha, S.;

Osterman, A.; Begley, T. P. NAD biosynthesis: identification of the

tryptophan to quinolinate pathway in bacteria. *Chem. Biol.* **2003**, *10*,

1195–1204.

29. Dua, R. K.; Taylor, E. W.; Phillips, R. S. *S*-Aryl-L-cysteine *S,S*Dioxides:

Design and evaluation of a new class of mechanism

based inhibitors of kynureninase. *J. Am. Chem. Soc.* **1993**, *115*, 1264–

1270.

30. Walsh, H. A.; O'Shea, K. C.; Botting, N. P. Comparative inhibition

by substrate analogues 3-methoxy- and 3-hydroxydesaminokynurenine

and an improved 3 step purification of recombinant human kynureninase.

BMC Biochem. **2003**, *4*, 13.

31. Heiss, C.; Anderson, J.; Phillips, R. S. Differential effects of

bromination on substrates and inhibitors of kynureninase from

Pseudomonas fluorescens. *Org. Biomol. Chem.* **2003**, *1*, 288–295.

32. Fitzgerald, D. H.; Muirhead, K. M.; Botting, N. P. A comparative

study on the inhibition of human and bacterial kynureninase by novel

bicyclic kynurenine analogues. *Bioorg. Med. Chem.* **2001**, *9*, 983–

989.

33. Carpenedo, R.; Chiarugi, A.; Russi, P.; Lombardi, G.; Carla, V.; Pellicciari, R.; Mattoli, L.; Moroni, F. Inhibitors of kynurenine hydroxylase and kynureninase increase cerebral formation of kynurenate and have sedative and anticonvulsant activities. *Neuroscience* **1994**, *61*, 237–243.

34. Otwinowski, Z.; W., M. Processing of X-ray Diffraction Data Collected in Oscillation mode. *Methods Enzymol.* **1997**, *276,* 307-326..

35. McCoy, A. J.; Grosse-Kunstleve, R. W.; Storoni, L. C.; Read, R. J. Likelihood-enhanced fast translation functions. *Acta Crystallogr., Sect. D: Biol. Crystallogr.* **2005**, *61*, 458–464.

36. Murshudov, G. N.; Vagin, A. A.; Dodson, E. J. Refinement of macromolecular structures by the maximum-likelihood method. *Acta Crystallogr., Sect. D: Biol. Crystallogr.* **1997**, *53*, 240–255.

37. Lamzin, V. S.; Perrakis, A.; Wilson, K. S. The ARP/WARP suite for automated construction and refinement of protein models. In *International Tables for Crystallography, Volume F*; Kluwer Academic Publishers: Dordrecht, The Netherlands, 2001.

38. Emsley, P.; Cowtan, K. Coot: model-building tools for molecular graphics. *Acta Crystallogr., Sect, D: Biol. Crystallogr.* **2004**, *60*, 2126–2132.

39. Winn, M. D.; Isupov, M. N.; Murshudov, G. N. Use of TLS parameters to model anisotropic displacements in macromolecular refinement. *Acta Crystallogr., Sect. D: Biol. Crystallogr.* **2001**, *57*, 122–133.

40. Collaborative Computational Project, N. The CCP4 Suite: Programs for Protein Crystallography *Acta Crystallogr., Sect. D: Biol. Crystallogr.* **1994**, *50*, 760-763.

41. Davis, I. W.; Leaver-Fay, A.; Chen, V. B.; Block, J. N.; Kapral, G. J.; Wang, X.; Murray, L. W.; BryanArendall, W., III.; Snoeyink, J.; Richardson, J. S.; Richardson, D. C. MolProbity: all-atom contacts and structure validation for proteins and nucleic acids. *Nucleic Acids Res.* **2007**, *35*, W375–W383.

42. Cleland, W. W. Statistical analysis of enzyme kinetic data. *Methods Enzymol.* **1979**, *63*, 103–138.

43. Dalgliesh, C. E.; Mann, F. G. Synthesis of _-(3,4-dihydroxyphenyl)-*N*-methylserine (adrenalinecarboxylic acid). *J. Chem. Soc.* **1947**, 658–662.

44. Travis, B. R. S., M.; Hollist, G. O.; Borhan, B. Facile Oxidation of Aldehydes to Acids and Esters with Oxone. *Org. Lett.* **2003**, *5*, 1031–1034.

45. Acheson, R. M. B. D. A.; Brettle, R.; Harris, A. M. Synthesis of some acylglycines and related oxazolones. *J. Chem. Soc.* **1960**, 3457–3461.

CHAPTER 4

SUBSTITUTED S–ARYL–L–CYSTEINE SULFONE: MECHANISM BASED INHIBITOR

OF KYNURENINASE *

* Kumar, S.; Phillips, R. S. To be submitted to *Biochemistry*

4.1 Abstract

Carbinol and sulfonyl analogs of kynurenine are potent transition-state analogue inhibitors of bacterial kynureninase.[1,2] In contrast to bacterial kynureninase, 3-hydroxykynurenine is the preferred substrate for human kynureninase over L-kynurenine. Thus, potent inhibitors of human kynureninase must have an aromatic 3-hydroxy substituent. L-Cysteine sulfones are potent inhibitors of bacterial kynureninase, but are weak inhibitors of the mammalian enzyme[3]. The most potent of the above class of inhibitors is S-(2-aminophenyl)-L-cysteine sulfone with a K_i value of 30 - 70 nm.[1,2] The same compound has been tested against rat liver kynureninase and has a K_i of 18 μM and IC_{50} of 36 μM.[3] Synthesis of the sulfonyl analog of 3-hydroxykynureninase, S-(2-amino-3-hydroxyphenyl)-L-cysteine-S,S-dioxide, has been attempted and partially completed.

4.2 Introduction

Human kynureninase (EC 3.7.1.3) is a pyridoxal 5' phosphate (PLP) dependent enzyme that catalyzes the hydrolytic cleavage of 3-hydroxy-L-kynurenine to 3-hydroxyanthranilic acid and L-alanine[4] (Scheme 4.1). In prokaryotes, kynureninase preferentially catalyzes the cleavage of L-kynurenine to anthranilic acid and L-alanine (Scheme 4.2). The reaction is a key step in the catabolism of L-tryptophan by *Pseudomonas fluorescens* and some other bacteria.[2] The human kynureninase has also been cloned, expressed and purified[4]. The crystal structures of both the human and bacterial enzyme have been published and compared.[6,7] The *P. fluorescens* kynureninase is highly homologous to the human enzyme, with 28% identical residues.[6] In mammals, kynureninase is the third enzyme in the "kynurenine pathway" of

tryptophan metabolism, which is the major pathway for the hepatic catabolism of tryptophan and is responsible for the *de novo* biosynthesis of NAD^+ in the absence of niacin.[5-7] In extrahepatic cells, kynureninase is also expressed in macrophages and microglia cells and the primary metabolite in these cells is quinolinic acid, not NAD^+. However, quinolinic acid is also a neurotoxin, due to its agonist effects on the *N*-methyl-D-asparate receptor,[8] and excessive levels of quinolinate have been implicated in the etiology of a wide range of diseases such as epilepsy, stroke, and neurological disorders, including AIDS-related dementia.[9] Thus, inhibitors of kynureninase are of interest as possible drugs for the treatment of a range of neurological disorders.
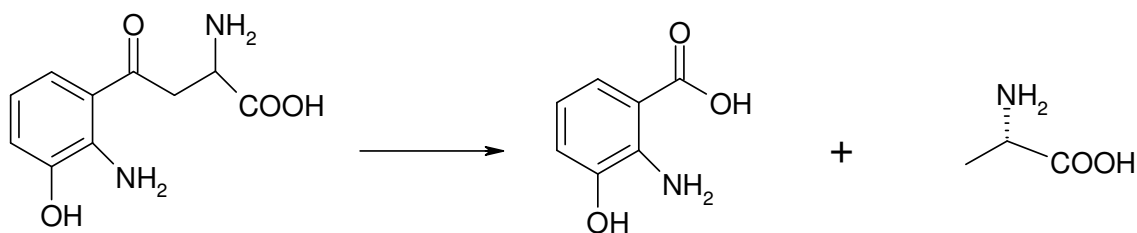
Scheme 4.1. Cleavage of 3-hydroxy-L-kynurenine by mammalian kynureninase
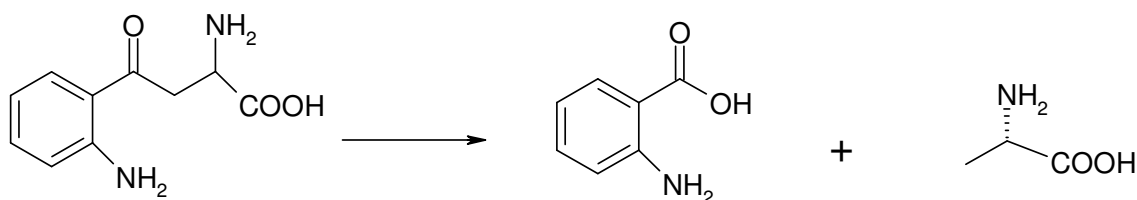

Scheme 4.2. Cleavage of L-kynurenine by mammalian bacterial kynureninase

Sulfonyl analogs of kynurenine are potent inhibitors of bacterial kynureninase. S-(2-aminophenyl)-L-cysteine S,S-dioxide has a Ki value of 30 - 70 nm against bacterial kynureninase.[1,2] The same compound has been tested against rat liver kynureninase

and has a K_i of 18 μM and IC_{50} of 36 μM.[3] The inhibition by this class of inhibitors is likely due to their structural similarity to the *gem*-diolate anion, a proposed reaction intermediate, in the reaction of kynurenine with kynureninase (Scheme 4.3). 3-Hydroxykynurenine is the preferred substrate for human kynureninase compared to L-kynurenine, because of the high K_m and low specific activity of L-kynurenine. To be a potent inhibitor of human kynureninase, the presence of an aromatic 3-OH substituent is important because of its involvement in hydrogen bond interactions with the aromatic residues at the active site of the protein.[10] Thus, we predict that S-(2-amino-3-hydroxy)-L-cysteine-S,S-dioxide could be a potent inhibitor for human kynureninase because of its close resemblance to 3-hydroxykynurenine, the natural substrate of human kynureninase.
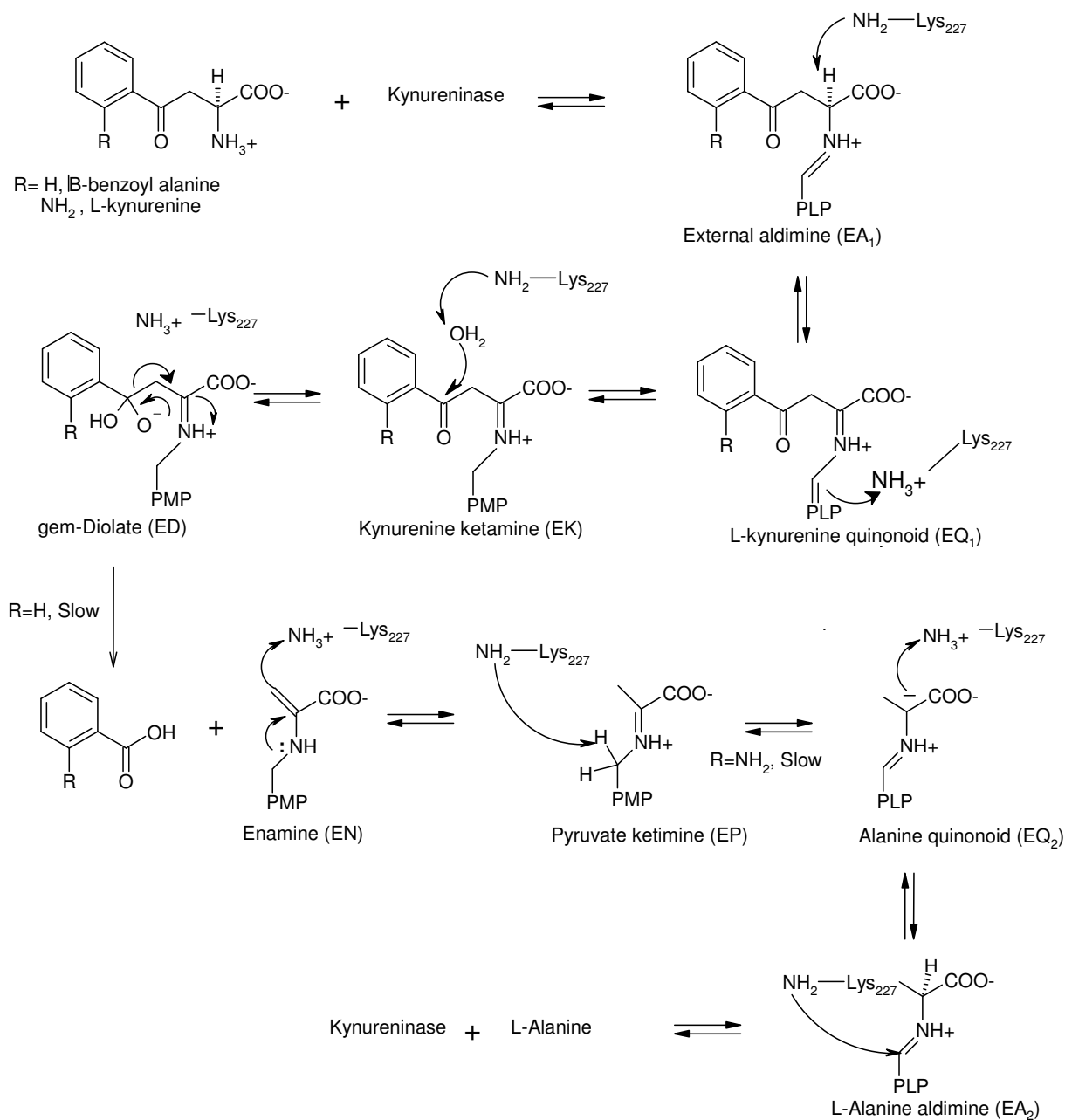
Scheme 4.3. Mechanism of reaction of bacterial kynureninase with β-benzoyl-

alanine.[11]

4.3 Results

Chemistry

The first step in the synthesis (Scheme 4.4) was nitration of 3-fluorophenol. Both the fluorine and hydroxyl are *ortho-, para-* directing groups so there are four possible sites on the aromatic ring for nitration. To obtain the nitration regioselectively at the 2-position of 3-fluorophenol, it was important to first block the other available *ortho-* and *para-* positions on the aromatic ring. To achieve this goal 3-fluorophenol was treated with oleum to obtain the 4-fluoro-6-hydroxybenzene-1,3-disulfonic acid **(3)** at the 4- and 6- positions of the ring.[12,13] Once the 4- and 6- positions were blocked with the sulfonate groups, nitration at the desired position was obtained by treating the 1,3-disulfonic acid **(3)** with a mixture of nitric acid and oleum. The nitration mixture was pre-cooled in an ice bath and was added slowly and dropwise to a ice cooled solution of compound **(3).** Temperature was never allowed to exceed 20°C. Hydrolysis of compound **(3)** in a jet of steam followed by distillation afforded 3-fluoro-2-nitrophenol **(4)** as a dark reddish liquid. The nitrophenol **(4)** was kept in the freezer for 24 hours and then re-crystallized with hexane/methanol as short red needle-like crystals. Compound **(4)** was then protected at the hydroxyl group using benzyl bromide and potassium carbonate to produce 1-(benzyloxy)-3-fluoro-2-nitrobenzene **(5)**. Since fluorine is present *ortho-* to the strongly electron-withdrawing nitro group, use of a strong base, like sodium hydroxide in the workup will displace the fluorine by nucleophilic aromatic substitution. In the next step, nucleophilic aromatic substitution of fluorine in 1-(benzyloxy)-3-fluoro-2-nitrobenzene **(5)** by L-cysteine yielded S-(2-nitro-3-benzyloxyphenyl)-L-cysteine **(6)** as a yellow solid.

Oxidation of compound **(6)** with a mixture of trifluoroacetic acid and hydrogen peroxide resulted in the formation of the sulfone, S-(2-nitro-3-benzyloxyphenyl)-L-cysteine S,S-dioxide **(7)**. The final step in the synthesis was the simultaneous reduction of the nitro group to the amino group and the deprotection of the benzyl ether to furnish S-(2-amino-3-hydroxy)-L-cysteine S,S-dioxide **(1)**. To achieve that 10% Pd/C was added to compound **(7)** and the mixture was hydrogenated for 2 h. The progress of the reaction was monitered by TLC. We got the product as confirmed by 1H NMR and mass spectroscopy, but I haven't got enough to purify it by column chromatography. The last step can be attempted by doing the reaction on a larger scale.
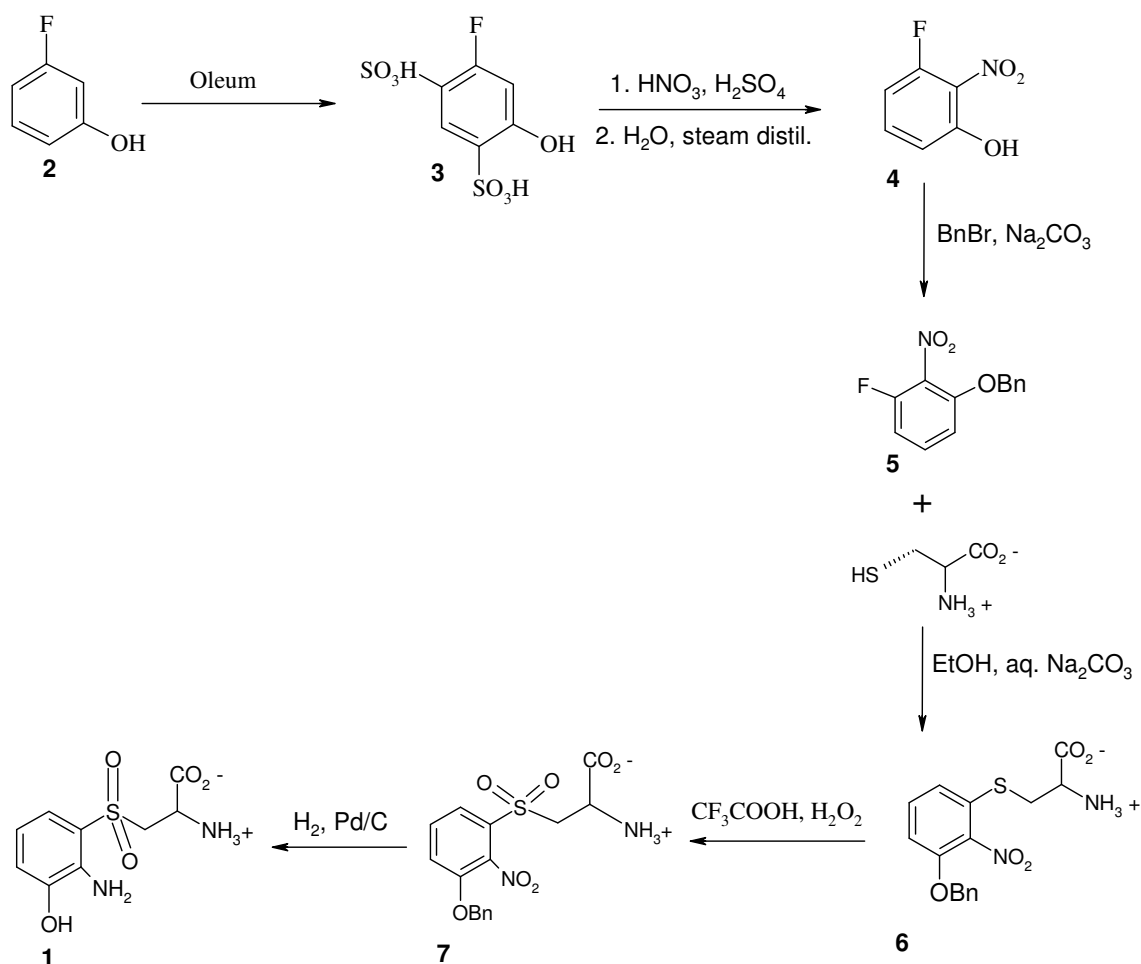
Scheme 4.4. Synthesis of S-(2-amino-3-hydroxyphenyl)-L-cysteine S,S-dioxide

4.4 Experimental procedures

Synthesis

3-Fluoro-2-nitrophenol (4)[12,13]

3-Fluorophenol **(2)** (4.6 ml, 5.6 g, 0.05 mol) was added slowly and drop wise to 20 ml of oleum (27 % SO_2, ρ = 1.94), in an ice bath. The mixture was kept overnight and then heated for 2 hours on a water bath to give 4-fluoro-6-hydroxybenzene-1, 3-disulfonic acid **(3)**. Compound **(3)** was not isolated and the reaction mixture was taken as it is for nitration. A cooled mixture of nitric acid (3 ml. ρ = 1.5) and oleum (10 ml, 27 % SO_2, ρ = 1.94) was then added dropwise with constant stirring to the above pre-cooled mixture. On dilution with 50 g of crushed ice and hydrolysis in a current of steam, 3-fluoro-2-nitrophenol **(4)** distilled out as a thick reddish oil. Compound **(4)** was kept in the freezer for 24 hours and then re-crystallized with hexane/methanol in short red needle-like crystals.

Yield 3 g (38 %), mp.= 39 °C.

^{1}H NMR ($CDCl_3$) δ (ppm)   6.95 (m, 1h), 7.06 (m, 1H), 7.65 (dd, 1H), 9.82 (s, 1H)

1-(Benzyloxy)-3-fluoro-2-nitrobenzene (5). A stirred mixture of 2-nitro-3-fluorophenol **(4)** (2.46 g, 0.016 mol), benzyl bromide (2.05 ml, 2.96 g, 0.017 mol), anhydrous potassium carbonate (2.21 g, 0.016 mol) in 20 ml of DMF was heated at 90 °C for 3 hrs. Most of the DMF was evaporated in vacuo. The oily mixture was then poured into 100 ml of 10 % sodium carbonate solution and extracted with ether (3 x 20 ml). The combined extracts were dried over sodium sulfate, filtered and evaporated to give yellow solid of 1-(benzyloxy)-3-fluoro-2-nitrobenzene **(5).** Compound **(5)** was then

recrystallized with methanol and cooled to 0°C to give bright yellow crystals. Yield 3.16 g (80 %).

^{1}H NMR (CDCl$_3$) δ (ppm)   5.16 (s, 2H), 6.71 (d, 1H), 7.06 (m, 1H), 7.11 (dd, 1H), 7.38 (m, 3H), 7.47 (m, 2H)

S-(2-Nitro-3-benzyloxyphenyl)-L-cysteine (6)[14]

A mixture of L-cysteine hydrochloride monohydrate (0.256 g, 1.46 mmol) and sodium bicarbonate (0.368 g, 4.38 mmol) in 4 ml of water was added to 1-(benzyloxy)-3-fluoro-2-nitrobenzene **(5)** (0.36 g, 1.46 mmol) in 10 ml of ethanol. The reaction mixture was refluxed for 3 hrs and then cooled to room temperature. The solids were removed by filtration and the solution was concentrated to 1/4th of the original volume and 10 ml of water was added. The aqueous suspension was washed with 20 ml of ether and acidified to pH 1 with 6N HCl. The resulting yellow precipitate was then vacuum filtered and dried over filter paper to give yellow solid of S-(2-nitro-3-benzyloxyphenyl)-L-cysteine hydrochloride **(6).** Yield 0.28 g (56%).

^{1}H NMR (D$_2$O + DCl) δ (ppm) 3.3 (dd, 1H), 3.5 (dd, 1H), 4.1 (m, 1H), 5.16 (s, 2H), 6.71 (d, 1H), 7.21 (m, 1H), 7.63 (dd, 1H), 7.38 (m, 3H), 7.47 (m, 2H)

S-(2-nitro-3-benzyloxyphenyl)-L-cysteine S,S-dioxide (7)[2]

S-(2-nitro-3-benzyloxyphenyl)-L-cysteine hydrochloride **(6)** (0.26 g**,** 0.74 mmol) was added to a solution of 5 ml of trifluoroacetic acid and 1 ml of 30% aqueous hydrogen peroxide. The solution was stirred overnight and the pale yellow solution was evaporated in vacuo at 30 °C. The oily residue was then triturated with water to give yellowish white crystals of S-(2-nitro-3-benzyloxyphenyl)-L-cysteine S,S-dioxide **(7)**.

Yield 0.18 g (64 %)

^{1}H NMR (D$_2$O + DCl) δ (ppm) 4.11 (m, 2H), 4.5 (m, 1H), 5.16 (s, 2H), 6.71 (d, 1H), 7.21 (m, 1H), 7.63 (dd, 1H), 7.38 (m, 3H), 7.47 (m, 2H)

S-(2-Amino-3-hydroxy)-L-cysteine S,S-dioxide[1] (1)

S-(2-Nitro-3-benzyloxyphenyl)-L-cysteine S,S-dioxide **(7)**.was dissolved in 10 mg 10% Pd/C and stirred in hydrogen atmosphere (balloon) for 2 h. The charcoal was removed by filtration through Celite, and the filtrate was concentrated in vacuo to give light tan oil. Purification of the compound has not been achieved yet. MS, [M+ Na]$^+$ = 283.0

^{1}H NMR (D$_2$O + DCl) δ (ppm) 3.77-3.98 (m, 4H), 4.65 (s, 2H), 6.9-7.85 (m, 6H).

4.5 Discussion

It has been reported that S-(2-aminophenyl)-L-cysteine S,S-dioxide has a Ki value of 30 - 70 nm against bacterial kynureninase and a K$_i$ of 18 μM and IC$_{50}$ of 36 μM against rat liver kynureninase.[14,7] Recently, the first ligand-complex structure at the active site of human kynureninase has been published[15], which shows that the hydroxyl group at the 3-position of the benzene ring of the ligand (3-hydroxyhippuric acid) is involved in important hydrogen bonding interaction with the carbonyl oxygen of Asn-333 at active site. This interaction was confirmed by mutant studies to be important for catalytic efficiency of human kynureninase. We hope that the 3-OH group in our target compound S-(2-amino-3-hydroxy)-L-cysteine S,S-dioxide **(1)** will play the same role. The synthesis of the final compound has already been completed but we have not succeeded in purifying it as a result of low yield. The purification of S-(2-amino-3-hydroxy)-L-cysteine S,S-dioxide **(1)** will be completed by the other members of Dr. R.S. Phillips group and will be tested as an inhibitor for human kynureninase.

4.6 References

1. Dua, R. K.; Taylor, E. W.; Phillips, R. S. *J. Am. Chem. Soc.* **1993,** *115*,   1264-1270.

2. Heiss, C.; Anderson, J.; Phillips, R. S. *Org. Biomol. Chem.* **2003,** *21*, 288-295.

3. Drysdale, M. J.; Reinhard, J. F. *Bioorg. Med. Chem. Lett.* **1998**, *8*, 133-138.

4. Shetty, A. S.; Gaertner, F. H. *J.Bacteriol.* **1975**, *122*, 235-244.

5. Soda, K.; Tanizawa, K. Adv. *Enzymol. Relat. Areas Mol. Biol.* **1979**, *49*, 1-40.

6. Momany, C.; Levdikov, V.;   Blagova, L.; Lima, S.; Phillips, R. S. *Biochemistry* **2004**, *43*, 1193-1203.

7. Lima, S; Khristoforov, R.; Momany, C.; Phillips, S. *Biochemistry* **2007**, *46*, 2735-2744.

8. Stone, T. W.; Perkins, M. N. *Eur. J. Pharmacol*. **1981**, *72*, 411-412.

9. Chiarugi, A.; Meli, E.; Moroni, F. *J. Neurochem.* **2001**, *77*, 1310-1318.

10. Lima, S.; Kumar, S.; Gawandi, V. B.; Momany, C.; Phillips, R. S. *J. Med. Chem.* **2009***, 52*, 389-396.

11. Gawandi, V. B.; Liskey, D.; Lima, S.; Phillips, R. S. *Biochemistry* **2004**, *43*, 3230-3237.

12. Hodgson, H. H.; Nixon, J. *J. Chem. Soc.* **1928**, 1879-82.

13. Hodgson, H. H.; Moore, F. H. *J. Chem. Soc.* **1925**, *127*, 1599-1600.

14. Slade, J.; Stanton, L. S.; David, D. B.; Mazzenga, G. C. *J. Med. Chem.* **1985,** *28*, 1517-1521.

Chapter 5

Conclusions

The goal of this research was to design and synthesize substrates and inhibitors for both bacterial and human kynureninase, which are required as drugs in the treatment of central nervous system (CNS) disorders. We also wanted to study the reaction of substituted β-benzoylalanine with kynureninase to determine if the *gem*-diolate (ED) formation or the retro-Claisen step to give the enamine (EN) is rate-determining in benzoate formation from β-benzoyl-L-alanine (Scheme 5.1).

In our study of the reaction between kynureninase and different substituted β-benzoylalanine, we obtained a downward curve in the Hammett plot of K_{cat}/K_0 against σ which is a result of change in the rate determining step with variation of substituent. According to the plot, the strongly electron-withdrawing substituent CF_3 favors the hydrolysis of *gem*-diolate intermediate and hinders the formation of hinders the cleavage of C_β-C_γ bond. The weakly electron-donating p-Cl which lies at the intersect of two opposite ρ values balances out the hydrolysis of *gem*-diolate and cleavage of C_β-C_γ bond.

Both the electron donating groups, p-Me and p-OMe, favor cleavage of the C_β-C_γ bond and hinder the attack of water molecule on the carbonyl group in (EK).

The ortho-substituted β-benzoylalanines which cannot be analyzed by the Hammett plot shows moderate activity with the enzyme. The ortho-Cl-benzoylalanine has a lower K_m

(7 μM) and a comparable K_{cat}/K_m (1.2 x 10^4) compared to benzoylalanine which has a K_m of 8 μM and k_{cat}/K_m equals to 8 x 10^4.

We also designed and synthesized hippuric acid analogs as inhibitors for human kynureninase. The 3-hydroxyhippuric acid has a K_i of 60 μM. Dr. S. Lima in our lab has obtained the crystal structure of 3-hydroxyhippurate bound in the active site of human kynureninase, which is the first substrate-enzyme crystal structure of kynureninase. This enzyme substrate complex can be used as a template for in silico design of more potent inhibitors, which will then be synthesized and evaluated.

We also attempted the synthesis of S-(2-amino-3-hydroxy)-L-cysteine S,S-dioxide which should be a good inhibitor of human kynureninase because of its resemblance to the natural substrate of human kynureninase, 3-OH kynurenine and to the intermediate *gem*-diolate (Scheme 5.1),.The synthesis of the final compound has already been completed but we have not succeeded in purifying it as a result of low yield. The purification of S-(2-amino-3-hydroxy)-L-cysteine S,S-dioxide will be completed by the other members of Dr. R.S. Phillips group and will be tested as an inhibitor for human kynureninase.
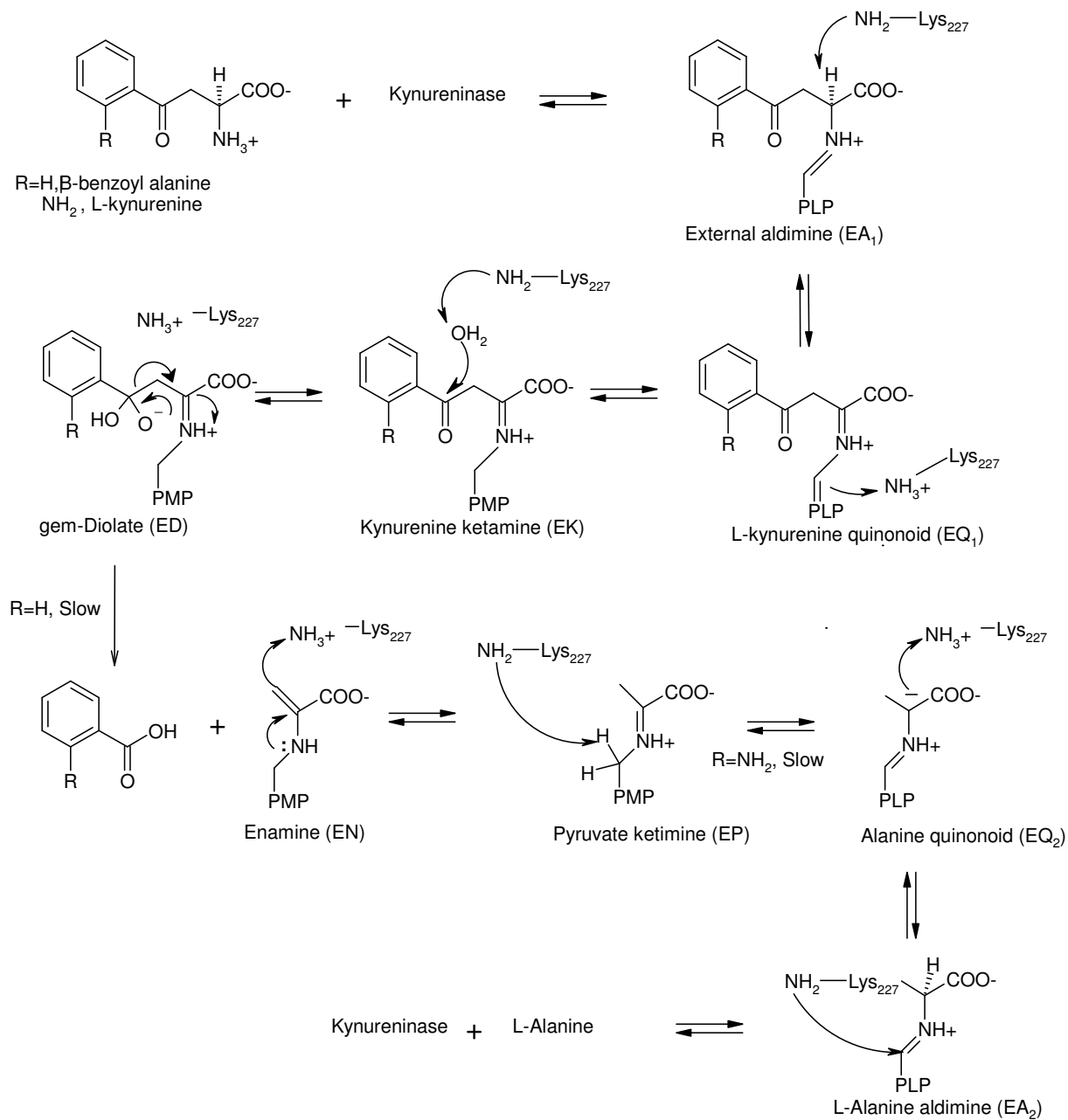
Scheme 5.1. Reaction of β-benzoylalanine and L-kynurenine with kynureninase.